# Modelling fluid flow in active clastic piercements: challenges and approaches.

M. Collignon[1], A. Mazzini[1], D.W. Schmid[2], Matteo Lupi[3].

1. Centre for Earth Evolution and Dynamics (CEED), Department of Geosciences, University of Oslo.
2. Physics of Geological Processes (PGP), Department of Geosciences, University of Oslo.
3. Department of Earth Sciences, University of Geneva, Switzerland.

**Abstract**

Clastic eruptions are the surface expression of piercement structures such as mud volcanoes or hydrothermal vent complexes and involve subsurface sediment remobilisation and fluid flow processes. During these eruptions, many different processes are involved over a wide range of temporal and physical scales, which makes it a highly challenging multi-phase and multi-processes system to model. Field studies on piercement structures rarely include monitoring and detailed descriptions of clastic eruptions, and only a few attempts have been made to model fluid flow during these events. Moreover, these models have usually only considered one or two dimensions and/or have a limited spatial resolution.

In this paper, we summarise the elements that are relevant for modelling fluid flow during clastic eruption: the geometry of the system, the ascending material and the host rocks. We present the main challenges associated with the identification of processes and quantification of parameters. By analogy to magmatic systems, we suggest that the type of clastic eruptions could be controlled by the liquid-gas flow pattern in the conduit. Effusive eruptions could be explained in terms of annular flows, while slug or churn flows could be expected during explosive events. We also propose that the viscosity of liquid mud controls the presence of slug flows in the conduit.

We then review the two main approaches that have been proposed to model the flow dynamics in the active conduits, Darcy and Navier-Stokes, as well as their key parameters and their validity.

Finally, we discuss the limits of the previously employed models and suggest further work directions to improve our understanding of clastic eruptions.

Keywords: clastic eruptions, modelling, mud volcanoes, sediment-hosted hydrothermal systems, fluid flow.

## 1. Introduction

The term piercement structures refers to a large group of geological phenomena among which are included diapiric bodies, mud volcanoes, hydrothermal vent complexes, and sediment-hosted hydrothermal systems (Fig. 1). The conduits of such active systems present complex dynamics involving deformation, brecciation, and transport of the sedimentary host rocks by ascending fluids (gas and/or liquids). Clastic eruptions are the surface expression of piercement structures that developed in the subsurface. These eruptions manifest themselves by the vigorous expulsion of clasts and fine grained sediments that are entrained by the upwelling fluids through the conduit. This mixture of rock clasts and fluids is called mud breccia. Clastic eruptions are driven by pore fluids overpressure and can be divided into two categories (Mazzini and Etiope, 2017):

1. Eruptions associated with purely sedimentary systems (Fig. 2a) that are driven by a combination of i) density inversion, resulting from differential compaction and high sedimentation rates, and ii) overpressure from catagenesis in organic-rich sediments in addition to that from intersected reservoirs. Mud volcanoes are surface examples of such sedimentary structures (Milkov, 2000; Aliyev et al., 2002; Dimitrov, 2002; Kholodov, 2002; Kopf, 2002; Etiope and Milkov, 2004; Mazzini, 2009; Bonini, 2012).
2. Eruptions associated with sediment-hosted hydrothermal systems (SHHS, or hybrid systems, Fig. 2b). Here the purely sedimentary processes (i.e. described above in point 1) are combined with the migration of deeper seated hydrothermal fluids that form in sedimentary basins when magmatic sills intrude organic-rich sedimentary rocks. This mechanism causes rapid heating of pore fluids and the organic matter in sediments. This results in pore fluid expansion (Jamtveit et al., 2004), metamorphic dehydration reactions and production of large quantities of gas (typically $CH_4$ and $CO_2$. Hydrothermal vent complexes and SHHS are surface examples of such systems (Welhan and Lupton, 1987; Bell and Butcher, 2002; Jamtveit et al.,

2004; Lee et al., 2006; Svensen et al., 2006; Svensen et al., 2009a; Mazzini et al., 2012; Iyer et al., 2013; Berndt et al., 2016; Ciotoli et al., 2016; Iyer et al., 2017).

Although mud volcanoes and SHHS have diverse origins and physical scales, they show structural and morphological similarities consisting in circular pipes (Fig. 2), which contain intensively deformed rocks, with a chaotic internal structure (e.g., Planke et al., 2003; Svensen et al., 2003; Roberts et al., 2010). Gases released at mud volcanoes are commonly methane-dominated, while SHHS are usually carbon dioxide-dominated (Mazzini and Etiope, 2017, Mazzini et al., 2007). Both systems represent pathways to the atmosphere for gases ($CO_2$, $CH_4$) produced at depth, which have the potential to drive global climate changes (e.g.,Judd et al., 2002; Kopf, 2003; Milkov et al., 2003; Etiope and Milkov, 2004; Svensen et al., 2004; Svensen et al., 2007; Etiope, 2015). Therefore, studying processes responsible for the formation of such systems and their eruption dynamics may help to better understand the causes of abrupt climatic and environmental changes (Wignall, 2001; Kvenvolden and Rogers, 2005; Svensen et al., 2009b).

Volcanic eruptions have been extensively studied for decades and well classified based on their eruptive mechanism and their intensity (Walker, 1973; Wilson et al., 1980; Hewhall and Self, 1982; McNutt, 1996; Sigurdsson et al., 1999; Thordarson and Larsen, 2007; Bonadonna and Costa, 2013, among many others). In contrast, clastic eruptions are poorly investigated and no such detailed classification is available for mud volcanoes or SHHS. A few studies have attempted to classify the eruptions of mud volcanoes based on their activity (Guliev, 1992; Fowler et al., 2000; Graue, 2000):

1. *Explosive*: powerful explosions of large volume of argillaceous material with numerous clasts and powerful flow of gas that spontaneously ignites. These eruptions are usually short but intense.
2. *Effusive*: emission of large amounts of low-viscosity mud breccia without intense gas emissions and explosions.
3. *Extrusive*: slow extrusion of viscous mud with negligible emission of gas.

Systematic monitoring and classification of the SHHS activity is complex and sporadic. Recently Karyono et al. (2017) recorded and described several phases of eruption activity for an active SHHS in East Java, Indonesia. While one of this phase (*regular bubbling activity*) is characterised by regular emissions of mud breccia and little amount of gas, another (*enhanced bubbling with intense vapour*) is characterised by intense vigorous mud bursting, accompanied by a noisy and vigorous degassing discharge and a dense plume that may rise up to 100 m above the ground. Mud volcano eruptions typically last from a few hours up to several days (Schnyukov et al., 1986; Aliyev et al., 2002; Deville and Guerlais, 2009; Mazzini and Etiope, 2017), while SHHS (e.g., hydrothermal vent complexes) have a longer erupting activity (e.g., Campbell, 2006; Mazzini et al., 2012).

Clastic eruptions have only been qualitatively described and no studies have tried to relate the type of eruptions to physical mechanisms, such as fluid flow, occurring at depth. Only a few attempts have been made to model fluid flow in active clastic piercements (Gisler, 2009; Mazzini et al., 2009; Zoporowski and Miller, 2009; Nermoen et al., 2010; Davies et al., 2011; Rudolph et al., 2011; Iyer et al., 2017). These models are limited in resolution and/or remain in one or two dimensions, and require much better constraints on the parameters and processes of erupting systems. As an example, numerical models that attempted to predict the longevity of clastic eruption (e.g., Davies et al., 2011; Rudolph et al., 2011) tend to overestimate or underestimate the duration of the eruption, reflecting limited information regarding the plumbing system.

In this paper, we review the main challenges in modelling fluid flow in active piercements and the approaches that have been taken in previous studies to model clastic eruptions. We only focus on the aspects concerning fluid flow during eruptions and not on the mechanisms of formation or pressure build up in these systems. We first list the elements to consider when modelling clastic eruptions and present the main challenges associated with the identification of processes and quantification of parameters. We then summarise the approaches that have been proposed to model clastic eruptions, followed by a discussion of their limitations and further research directions.

## 2. Elements of a model of clastic eruptions

Numerous parameters and processes need to be considered when modelling fluid flow in active systems. The ascending fluids can be at high temperature, pressurised, super-heated and even at critical state at depth. Fluids, which may have a shallow or deep origin, can in addition be confined by a cap or sealing unit until it breaches. Deformable and porous rocks are affected by ascending fluids. The rock clasts inside the conduit, resulting from the brecciation of host rocks during the fluid ascent is entrained by the fluids and propelled to the surface. Finally, the ascending fluids that may include both a gas and liquid phase, escape from the vent at the surface. Clastic eruptions are thus multiphase and multi-process systems. Hence models of clastic eruptions should consider the geometry of the systems (i.e. number, depth and size of reservoirs, conduit length and diameter), the ascending material (fluids and/or solid) and the host rocks. In the following sections, we separately discuss these three elements and the challenges associated to their modelling and/or characterisation.

### 2.1. Geometry of the system

The structural geometry of the plumbing system associated with piercements is complex. It integrates many aspects and parameters such as the conduit, the reservoir(s) of fluids and the network of fractures and pores (see section 2.3 on the host rocks) for the fluids to flow. The size and the interconnection of fractures, the main conduit radius, and the depth of reservoirs highly influence the fluid discharge, whereas the size of the reservoirs determines the amount of fluids that can be expelled. It is therefore challenging to include in numerical models all the parameters and the geometries characterising such systems.

Inevitably, assumptions and simplifications have to be made. When modelling clastic eruptions, a simplified geometry is often considered and consists of a reservoir with a single conduit connecting to the surface (Zoporowski and Miller, 2009; Davies et al., 2011; Rudolph et al., 2011). In such models, the geometry and depth of the reservoir, as well as the radius of the conduit, are essential parameters controlling the dynamics of mud flow. The radius is particularly difficult to constrain.

Even when a diameter of the surface vent can be inferred, it is difficult to speculate about the size of the conduit at depth (e.g., Planke et al., 2005; Huuse et al., 2010). The main feeder channel is supposedly wider at shallow depths due to gas expansion, fluidisation, and erosion of the host rocks and it gradually narrow with depth (Nermoen et al., 2010). Fluidisation processes during eruptions have been simulated with analogue models (Nermoen et al., 2010). Results show that vent sites have a subsurface conical shape whose angle to the vertical is consistent with the internal friction angle of the host rock. Therefore, it is theoretically possible to estimate the depth at which fluidisation and thus widening of the conduit occur.

Piercement structures can be identified using seismic imaging (Planke et al., 2005; Huuse et al., 2010; Moss and Cartwright, 2010). Though, due to the presence of fluids in and around the conduit, the seismic reflectors appear blurred, often over a wide part (~ 100-200 m), leading to an overestimation of the conduit width (see Huuse et al., 2010 for discussion). Previous studies showed that the conduit diameter has a dramatic effect on the mud discharge, and therefore suggested that an unconfined system with conduits in the range of a hundred metres is not plausible because the mud discharge will be unrealistically high (Lance et al., 1998; Kopf and Behrmann, 2000). The width of the main vent thus remains a difficult parameter to constrain, but it is nevertheless possible to determine a range of acceptable values (up to a few metres), once the discharge and properties of the fluid are known (Kopf, 2002; Collignon et al. 2017).

The depth and volume of the fluid source(s) are difficult to infer from the surface morphology of piercement structures but can be estimated by geophysical methods (Fukushima et al., 2009; Istadi et al., 2009; Aoki and Sidiq, 2014; Mordret et al., 2015; Shirzae et al., 2015; Obermann et al., 2016). One approach relies on linear elasticity theory (Mogi, 1958), and considers that ground deformation is a function of extrusion of material at depth (i.e. reservoir depletion). It is therefore possible to link the depth and volume of reservoir to the ground deformation under the assumption of a simplified geometry where the reservoir is a sphere whose radius is much smaller than the distance from the reservoir centre to the surface (Mogi, 1958; Fukushima et al., 2005; Shirzae et al., 2015). This method does not easily allow for the identification of several reservoirs, which may be stacked on top of each other. Field studies show a direct link between the morphology of the structures at the surface and the conduit radius, the physical properties of the expelled fluid, or even the depth of intruding magmatic sills (Lance et al., 1998; Kopf, 2002; Planke et al., 2005). Planke et al. (2005) highlighted that for hydrothermal vent complexes there is a general correlation between the size and geometry of their upper part and the mean depth to the sill intrusion. Shallow sill intrusions generate small, dome-shaped and eye-shaped upper parts on the surface, while large crater-shaped upper parts (> 5 km) are produced by deep sill intrusions. The size (and volume) of mud volcanoes is mainly a function of the size of the conduit, the driving forces of the eruption and the consistency of mud, as well as the frequency of eruptions (Kopf, 2002; Mazzini and Etiope, 2017). Wide conduits and an efficient trigger at depth tend to produce larger mud volcanoes. Mud domes or ridges are formed by muds with low porosities (< 50%) and more cohesive muds with intermediate fluid content can result in volcanoes with large diameters (1-2 km) and high elevations above the seafloor (> 50 m) (Lance et al., 1998). These relations between surface morphology and size and depth of the sources have been only qualitatively described but have not been quantified yet.

## 2.2. The ascending material

The ascending material generally consists of fluids, mostly mud (considered here as a liquid), carbon dioxide, methane and possible oil from hydrocarbon reservoirs, as well as of rock fragments. Models should ideally consider the flow of several phases and the physical properties of each one of them. Properties include, among others, density, viscosity, clay content in liquid mud, temperature. These parameters are not independent, but intrinsically linked and influence each other (e.g. clay content and temperature influence both the viscosity and density of the mud). In this section, we discuss multiphase flows, rheology and density of the ascending materials.

### 2.2.1. Multiphase flow

*Phase definition*

A phase is a material whose physical properties are homogeneous in space. The term phase can sometimes refer to state of matter (i.e. solid, liquid, gas or plasma), but there can also be several immiscible phases of the same state of matter (e.g., oil and water are two immiscible phases of the same state of matter, the liquid). Fluid mechanics considers multiphase flow as the simultaneous flow of 1) a material with different state of matter or 2) a material with different physical properties but in the same state of matter (e.g., oil droplets in water represent a two-phase liquid-liquid flow). For multiphase flow, a phase is considered as a component that is chemically uniform and physically distinct (i.e. immiscible). However, each phase can be composed of several miscible components (e.g., methane, carbon dioxide or aqueous vapour for a single gaseous phase).

Up to four immiscible phases (i.e. oil, mud, gas (e.g., $CO_2$, $CH_4$, $H_2O_{(v)}$) and solid rocks) can be present during clastic eruptions. Oil is usually the minor phase. Depending on the clast concentration and size, oil and rock clasts could be neglected and the ascending material will then be considered as a liquid-gas flow. If the emissions of gases are small compared to the ejection of mud breccia, the ascending material reduces to a solid-liquid flow (slurry flow). For large emission of gases and mud breccia, with abundant and large rock fragments, the ascending material should be considered as a gas-solid-liquid flow (gas-slurry flow).

*Flow pattern*

In multiphase flows the geometric distribution or topology of the phases can strongly affect the flow within each phase or component, the mass, momentum and energy rates, and processes taking place across the phase interface (Wörner, 2003; Brennen, 2005). It is therefore important to know the geometric distribution, or flow pattern, of the phases to model their flow accurately. Many studies have focussed on determining the patterns for various pairs of fluids, pipe geometry and inclinations primarily because of the numerous industrial and practical applications (Wallis, 1969; Taitel et al., 1980; Weisman, 1983; Barnea, 1987; Storkaas and Skogestad, 2007; Wörner, 2012 among many others). When modelling the dynamics of clastic eruptions, fluid flow in the shallow part of the system should be of interest. Usually the geometry, if unknown, is considered to be a vertical and circular conduit or pipe. We will focus mainly on the liquid-gas flow in vertical pipes as it has been amply studied experimentally and numerically for the industry (e.g., Taitel et al., 1980; Pickering et al., 2001; Taha and Cui, 2006; Storkaas and Skogestad, 2007) and later extrapolated to magmatic systems to explain some of the eruption types (e.g., Vergniolle and Jaupart, 1986; James et al., 2009; Pioli et al., 2012). Further details on flow patterns for different type of fluids and inclination pipes can be found in dedicated literature on multiphase flow (e.g. Weisman, 1983; Wörner, 2003; Brennen, 2005).

Flow pattern have been initially defined by visual inspection of laboratory experiments that sought to determine the dependence of the flow pattern on component volume fluxes, volume fraction, fluid properties (density, viscosity, surface tension) and pipe diameters (Wallis, 1969; Taitel et al., 1980; Barnea, 1987). Researcher have often displayed their results in form of regime maps that identify the flow patterns as a function of component flow rates (*superficial velocities*, defined as the ratio of the volume flow rate to the cross-sectional area, or *superficial momentum flux*, defined as the product of the density and the liquid volumetric flux to the power two) for given fluid properties and pipe diameters (Fig. 3). Hewitt (1999) categorised the flow pattern into three main types: dispersed, separated and intermittent flows. Dispersed flows, such as bubbly flows, consider all flow regimes where one phase is uniformly distributed as droplets throughout another continuous phase. In separated flows (e.g. stratified flows in horizontal tubes), phases are not mixed. Finally, intermittent flows apply when the phases are not distributed uniformly along the pipe, such as slug or plug flows. The four main basic patterns in vertical two phase flow have been visually identified as (e.g. Taitel et al., 1980):

1. *Bubble flow*. The gas is uniformly distributed as droplets in a continuous liquid phase (Fig. 3).

2. *Slug flow*. With increasing superficial gas velocities, bubbles tend to merge together to form large bullet-shaped bubbles whose diameter almost equals to the pipe diameter (Fig. 3). These bubbles, referred as Taylor bubbles, move uniformly upward and are separated by slugs of continuous liquid, which bridge the pipe and contain small gas bubbles. The liquid, between Taylor bubbles and the pipe wall, flows downward forming a thin falling film.
3. *Churn flow*. This flow is similar to the slug flow, although it is more chaotic, bubbly and disordered. The Taylor bubbles, present in the slug flow, are now narrower and their shape are distorted (Fig. 3). A high local gas concentration in the slug repeatedly destroy the continuity of the liquid between two distorted Taylor bubbles. When this happens, the liquid slug falls. This liquid then accumulates, forms a bridge and is lifted by the gas. These sequences of upward and downward motion of the liquid are typical of the churn flow.
4. *Annular flow*. This flow is characterised by the continuous flow of the gas phase along the pipe in its core. A part of the liquid phase moves upward, as a thin wavy liquid film along the pipe wall whereas the other part is entrained as droplets in the gas core (Fig. 3).

Transitions from bubble, to slug, to churn, to annular flow are obtained by progressively increasing gas superficial velocity (Fig. 3). Boundaries between patterns in flow maps have been initially defined experimentally in a two-dimensional coordinate systems, and are often represented as a line that is a function of the component flow rates. The flow may also be chaotic and the identification of the flow pattern difficult, leading to uncertainties in the identification of the boundaries. Transitions between patterns are controlled by the flow as well as features such as the roughness of the walls and the entrance conditions and are rather unpredictable. Hence, the flow pattern boundaries are not distinctive lines but rather poorly defined transition zones. Over the last four decades, substantial research has been dedicated to predict transitions from one regime to another in terms of physical mechanisms and dimensionless parameters (Wallis, 1969; Clift et al., 1978; Taitel et al., 1980; Barnea, 1987; Cheng et al., 2002). These studies have been partly motivated by the application of flow pattern in oil industry. Indeed, transitions from slug to annular flow is accompanied by pressure variations, leading to flow instabilities that are often experienced in many offshore platforms (Pickering et al., 2001; Toma et al., 2006; Campos et al., 2015). Unstable flows result in poor separation causing potential damage to critical equipment, resulting in high maintenance costs. To minimise pressure drop, a slug flow pattern is mainly used for gas lifting of relative large volumes of fluid (oil and water) while an annular flow pattern is preferred for the production of gas with relatively small amounts of condensate or water (Toma et al., 2006). The flow of injected gas can be controlled to ensure that the flow is stable within one or the other flow domain and to avoid any transition. However, this procedure may result in a production decrease and/or high economical costs, or can be unsuccessful as the stability might be difficult to sustain. Therefore, further studies of the flow patterns and their transitions are required to reduce the production costs.

The physical mechanisms by which transitions occur are different form one pattern to another. The transition from bubbly to slug flow is explained through the competing effects of bubble break-up and coalescence, which depend on surface tension and turbulence effects (Taitel et al., 1980). Bubble density increases together with the gas superficial velocity, leading to an increase in the coalescence rate. However, if the liquid velocity increases, large bubbles, formed by coalescence of small bubbles, may break up due to turbulent fluctuations associated with the flow. At low liquid velocity, and with increasing gas superficial velocity, there is a point reached where dispersed bubbles become so closely packed that the rate of coalescence increases sharply, leading to a transition to slug flow. This transition was observed in experiments for gas volume fractions around 0.25 to 0.30. The maximum size of a stable gas bubble for bubbly flow has been investigated as a function of turbulence effects by many authors (e.g. Brodkey, 1967; Taitel et al., 1980; Ohnuki and Akimoto, 2000; Guet et al., 2002; Omebere-Iyari et al., 2007). The churn flow is characterised by oscillatory motion (upward and downward) of the liquid between two successive Taylor bubbles. Taitel et al. (1980) define the churn flow as an entrance phenomena that may occur if the pipe length is not long enough for slug flow to develop. Indeed, in experiments where stable slug flow developed higher in the tube, the authors still observed some repeated upward and downward motions of the liquid at the inlet. They developed a method for calculating the entry length required to develop stable slug flow and proposed that the distance from the entrance to that length is where churn flows can be observed. Annular flow cannot exist unless the gas velocity in the gas core is sufficient to lift the entrained droplets. The minimum gas velocity required to suspend a drop is determined from the balance between the gravity and drag forces acting at the drop (Taitel et al., 1980). Taitel et al. (1980) and later other authors (e.g. Barnea, 1987; Ohnuki and Akimoto, 2000; Guet et al., 2002; Omebere-Iyari et al., 2007) proposed some equations for the different transitions. However, some of these equations are only valid for small pipe diameters (e.g. bubble – slug transition), as other processes may be dominant for large diameters (Cheng et al., 1998; Pickering et al., 2001; Omebere-Iyari et al., 2008; Pioli et al., 2012). Moreover, one transition may occur at a critical Weber number (e.g. slug - annular), whereas another boundary may be characterised by a particular Reynolds number (e.g. bubbly - slug) (Brennen, 2005). To sum up, there is no universal dimensionless flow pattern map that incorporate the full parametric dependence of the boundaries on the fluid characteristics.

*Application to natural systems*

Previous studies showed that the separation of exsolving gases from low viscosity magma can produce different eruption styles that could be explained in term of two phase flow regimes (Vergniolle and Jaupart, 1986; Jaupart and Vergniolle, 1989; Parfitt, 2004; James et al., 2008). For example, Strombolian eruptions have been explained in term of slug flow whereas annular flows are expected for Hawaiian eruption (Vergniolle and Jaupart, 1986; Jaupart and Vergniolle, 1989). Transition from one pattern to another have been thought to cause rapid changes in eruption styles (e.g. from pulsatory to continuous activity or variations in explosivity) (Parfitt, 2004; James et al., 2009; Lyons et al., 2010). For low-viscosity basaltic magmas, the stability and characteristics of two-phase flow pattern have been mostly predicted from a combination of theoretical studies and experiments with air-water fluids in small pipe diameters (e.g. Taitel et al., 1980; Barnea, 1987; Taha and Cui, 2006). Therefore, the application of the results to magmatic systems are only valid for specific aspects of the flow dynamics in conduit. Pioli et al. (2012) investigated the effects of outgassing of basaltic magma on the flow dynamics in conduit, using glucose syrup-air and water-air experiments in large pipe diameter (0.24 m). They predicted an increase in magma vesicularity (void) with increasing gas superficial velocity, reaching a maximum value of ~ 0.45 in volume. This value corresponds to the expected conditions for annular flow that the authors estimated to occur at minimum values of $10^3$-$10^4$ $m^3s^{-1}$ for the gas volume flow rate. Their study, however, does not account for gas exsolution and expansion near the surface, which can generate large burst (James et al., 2008).

Clastic eruptions, in comparison, are poorly described and no relation between the eruption style and two phase flow patterns has been proposed. Hence, any prediction for clastic systems of the two-phase flow patterns as a function of dimensionless parameters (Froude, Morton, Eötvös), as proposed for magmatic systems (e.g., James et al., 2004; Pioli et al., 2012), will be highly speculative. Nevertheless, some analogies could carefully be done with magmatic systems and experimental studies to relate the eruption styles of clastic systems with the flow patterns in the conduit, and the depth at which these patterns could potentially exist. Strombolian eruptions consist in a series of discrete explosions, characterised by large gas bubbles bursting near the surface, whereas Hawaiian eruptions are more effusive, characterised by fire fountains that are driven by gas jets in the centre (Vergniolle and Jaupart, 1986). We thus speculate that explosive mud volcano eruptions could be explained in term of slug or churn flow patterns while annular flows could be expected for the effusive mud volcano eruptions. The slow extrusive eruptions, observed for mud volcanoes, could be controlled by a bubbly flow in the conduit. The different eruption styles observed by Karyono et al. (2017) for the Lusi mud eruption, from regular bubbling to enhanced bubbling with intense vapour suggest an increase in gas content. By analogy to magmatic systems, these changes in eruption styles could be explained in term of transitions of the flow patterns in the conduit from bubbly to annular flows. These speculations are only valid if we consider a system which is mud dominated (negligible clast content) and for which the viscosity is close to the one of low viscosity basaltic systems. Indeed, the stability of two-phase flow patterns is strongly controlled by the liquid viscosity, both in term of conditions and observed patterns (Pioli et al., 2012). As an example, the slug flow pattern, characterised by the presence of Taylor bubbles, was not observed in water-air experiments for larger diameters (> 10 cm) because large bubbles are instable due to inertial forces (Pickering et al., 2001;

Pioli et al., 2012). Slug flows were, however, observed in glucose-air experiments and are expected in volcanic systems, where the viscosity of the liquid phase is higher (Vergniolle and Jaupart, 1986; James et al., 2011; Pioli et al., 2012). The viscosity of liquid mud is complex and can vary a lot as a function for example of the water content. Mud with a high-water content (> 0.8 in mass) will have a low viscosity, closer to water than magma. The size of the conduit of clastic systems, often unknown, has been estimated not to exceed a few metres, but probably to be larger than a few tens of centimetres, based on extruded rock fragments. Therefore, we can predict that for mud with a high-water content, the slug flow pattern will not be present in the conduit.

Transition from one pattern to another depends, among other parameters, on the gas volume fraction. Bubble coalescence, and thus slug flows do not develop for gas volume fraction smaller than 0.2 while annular flows develop above 0.75 (Taitel et al., 1980; Vergniolle and Jaupart, 1986; Cioncolini and Thome, 2012). During clastic eruptions, the gas volume fraction in the rising mud increases due to gas exsolution and expansion at lower pressures. If the proportion of gas and liquid through a vertical conduit is known, it is then possible to estimate at which pressures, and thus depths, the transitions between flow pattern occur. Figure 4 shows an idealised evolution of liquid-gas flow pattern in a vertical boiler tube. The transition from a single-phase liquid flow to a two-phase bubbly flow occurs when the gas phase, dissolved at deeper depths, starts to be freely released in the liquid phase. This transition is controlled by the solubility of the gas and greatly depends on the physical and chemical properties of both the gas and liquid, as well as on pressure, temperature, salinity and pH of the solution. The depth at which this transition will occur depends on the nature of the gas and its initial concentration in the system. In clastic eruption, the main gases expelled, besides aqueous vapour, are carbon dioxide and methane. The binary systems $CH_4$-$H_2O$ (e.g., Yamamoto et al., 1976; Duan and Mao, 2006; Guo and Rodger, 2013) and $CO_2$-$H_2O$ (e.g., Diamond and Akinfiev, 2003; Duan and Sun, 2003; Chapoy et al., 2004; Mao et al., 2013) have been intensively studied, and $CO_2$ and $CH_4$ solubilities in water are well constrained for a wide range of temperatures and pressures. However, the ternary system $CO_2$-$H_2O$-$CH_4$ was only experimentally constrained for a limited range of temperatures and pressures (e.g., Qin et al., 2008). Natural fluids are more complex and the presence of other elements may modify the solubility. For example, the presence of NaCl in an aqueous solution tends to reduce the solubility of methane and carbon dioxide for the $H_2O$-$CH_4$ and $H_2O$-$CO_2$ binary systems respectively (e.g., Duan and Sun, 2003; Duan and Mao, 2006). Experimental data showed that $CH_4$ becomes more soluble in the presence of $CO_2$. The measured $CH_4$ solubility in the ternary mixture is 10 to 40% (for T~375K and 10 < P < 50 MPa) more than what was calculated for the binary system $H_2O$-$CH_4$ (Qin et al., 2008). Ideally, the solubility of each component should be known to be able to predict how many phases are present as a function of temperature and pressure. However, it is difficult to measure and predict the solubility of a gas over a wide range of temperatures and pressures for a system with more than three or four components, and models usually tend to consider only two, or three at most components in the gas phase.

Using a simple model, we roughly estimate the transition between the different patterns in terms of gas volume fraction and solubility for a mud with methane as well as for a mud with carbon dioxide. The solubility of carbon dioxide and methane were calculated from the models of Duan and Sun (2003) and Duan and Mao (2006), respectively. In both cases, we consider an initial concentration of 1 mole per kilogramme of water and a mud temperature of 60ºC (average temperature for clastic systems). We consider that the eruption is fast and that the fluids do not have the time to cool down. The mud has a water content of 0.5, a density of 1500 kg $m^{-3}$, and a zero salinity. The gas volume fraction is defined as:

$$\alpha = \frac{V_g}{V_g + V_l}, \quad (1)$$

with $V_g$ and $V_l$ the volume of gas and liquid, respectively, and $V_g = \frac{nRT}{P}$. In our model, we consider that the reduction of liquid volume with pressure is negligible compared to the reduction of gas volume, and the liquid volume is thus kept constant. We calculate the gas volume fraction and solubility for pressures from 0 to 500 bar, which roughly corresponds to depths from 0 to 3.5 km. Methane is present as free gas over this range of pressure, and the flow pattern is at depth, bubbly flow. The transition from bubbly to slug flow ($\alpha$ ~ 0.2) patterns occurs around 80 bar, at a depth of ~ 500 m. The transition from slug to annular patterns is estimated around 7 bar, at a depth of ~ 50 m

(Fig. 4). In the case of the system liquid mud - carbon dioxide, the transition between a single phase and a two-phase bubbly flow occurs around 95 bar, at a depth of ~ 650 m. The transition from bubbly to slug flow is estimated around 40 bar, at a depth of ~ 250 m, while the transition from slug to annular flow occurs around 6 bar, at a depth of 40 m.

These values are more indicative than quantitative as the model used here is very simple and only considers the exsolution of a single gas ($CH_4$ or $CO_2$) with pressure reduction at a fixed temperature. Moreover, these transitions highly depend on the nature of the gas and its initial concentration in the system. Thus, for smaller concentration, these transitions will be shifted at shallower depths, and are expected to occur at greater depths for larger concentrations. If the temperature is higher, water can be in the gas phase, increasing the total gas concentration. Each system is specific and a general prediction of the depths at which these transitions occur is highly challenging. Nevertheless, as the transition are partly controlled by the gas volume fraction that strongly increases at low pressures, we suggest that the annular flow pattern is restricted to shallow depths, probably less than 100 m. If the gas concentrations are low, this pattern may not have the possibility to develop. These estimations have not yet been supported by field or experimental data for clastic eruptions and further work is required. Moreover, a cylindrical conduit geometry is likely only valid for the upper part of clastic piercements (Ryan, 1988; Keating and Valentine, 2008).

### 2.2.2. Rheology

Rheology is of crucial importance when modelling ascending fluids in eruptions. Rheology describes the behaviour of fluids, characterised by mathematical functions that relate stresses to strain rates (Mader et al., 2013, and Fig. 5). The viscosity is the resistance of a fluid against deformation and is a key parameter in fluid flow models. The rock fragments do not technically flow but are rather entrained by the ascending fluids (i.e. the mud and the gas). However, solid particles may influence the rheology of the fluids, depending on their concentration and shape (e.g. Ancey, 2001; Ovarlez et al., 2015). Ideally, the model should consider the influence of each phase on the rheology. This is difficult and simplification have thus to be done. Rock fragments can be modelled as rigid particles, by imposing a high viscosity, so that they are not deformed by the flow of the fluids. Usually, numerical or experimental models consider a simple geometry (sphere or prism) for the particles (e.g., Lecampion and Garagash, 2014; Yamato et al., 2015). In liquid-gas fluid flow the liquid viscosity is one of the parameter controlling the stability of flow patterns, rather than the gas viscosity. Gas viscosities are mostly depending on the temperature and are at least two to three orders of magnitude lower than the liquid viscosity. We will here discuss the liquid phase (mud), which in the case of clastic eruptions is a complex fluid with a high variability due to the nature and properties of clay minerals. Gas and solid phases can also be seen as parameters that influence the rheology of the mud, if considering a single-phase flow.

The mud viscosity is related, among other parameters, to the mud texture. Therefore parameters which influence the strength of aggregation bonds also affect the viscosity (Berlamont et al., 1993). These parameters are solid concentration, gas and water content, salinity, mineralogical composition, temperature, organic matter content, pH, and redox potential (Berlamont et al., 1993).

Mud is generally considered as a non-Newtonian fluid (i.e. it is not possible to define a single strain-rate-independent viscosity for such non-linear flow curves, Fig. 5), exhibiting a yield stress ($\tau_0$) which needs to be exceeded for flow to take place. The yield stress is partly affected by the solid volume fraction ($\phi$) (Locat and Demers, 1988; Major and Pierson, 1992; Coussot, 1995; Ancey and Jorrot, 2001). In addition, clay-water mixtures (muds) show a thixotropic behaviour (Toorman, 1997). Thixotropy is defined as "the continuous decrease of viscosity with time when flow is applied to a sample that has been previously at rest and the subsequent recovery of viscosity in time when the flow is discontinued" (Mewis and Wagner, 2009).

The structural breakdown (implying viscosity reduction) during shear involves two opposite processes. First, the applied shear tends to disrupt structured primary particles and/or aggregates (flocs) of such particles. Second, shear induced collisions of the separated elements tend to reform part of the broken bonds. The state equilibrium is reached when the bond-breaking and -forming rates balance (Toorman, 1997; Mewis and Wagner, 2009). Two approaches are usually taken to model thixotropy. The first considers models based on general principles of continuum mechanics that describes the time effects by means of memory functions (e.g., Stickel et al., 2007). The second approach introduces a structural parameter to model the time dependent rheological behaviour. This parameter expresses the instantaneous degree of structure having a value between 0 (fully broken) and 1 (fully structured). The model associates a rheological response to the instantaneous structure and the time dependence is expressed by a kinetic or evaluation equation for the structural parameter (Toorman, 1997 and references therein; Mewis and Wagner, 2009). Previous rheological studies showed that mud behaviour could be approximated using a Bingham (e.g., Locat and Demers, 1988; Toorman, 1994) or a Herschel-Bulkley (e.g., Coussot, 1994; Coussot and Boyer, 1995) flow formulation (Fig. 5).

The viscosity of liquid mud is reduced with increasing shear and also possibly with time. As a result, the velocity of the liquid increases in the conduit and the flow regime, or even the governing processes may change, depending on the magnitude of the viscosity reduction. Such variation in the flow regime could consequently modify the type of eruptions. For example, at low to moderate gas superficial velocity, an increase in the superficial liquid velocity could trigger a transition from the slug to bubbly flow (Fig. 3). If the viscosity is strongly reduced (close to water viscosity), inertial forces may dominate over viscous forces (James et al., 2004). Ideally, the model should take into account the correct rheology of the system for which parameters can be constrained experimentally.

*Measuring the viscosity of mud samples*

Rheological parameters for a mud sample can be derived from its experimental flow curve by using the best fitting model (e.g., Bingham or Herschel-Bulkley models). A rheometer measures the torque, which is proportional to the shear stress ($\tau$) at the rheometer wall (i.e. boundaries), as a function of the rotation speed, which is supposedly proportional to the shear strain rate ($\dot{\gamma}$). We can then define the apparent dynamic viscosity ($\eta$) that is obtained as the ratio of shear stress to shear strain rate intensity ($\eta = \tau/\dot{\gamma}$, Fig. 5) (Berlamont et al., 1993).

Although in theory the methodology employed to determine the rheological parameters of a mud sample is not complicated, many technical issues, such as sedimentation or ionic interaction, may occur in the laboratory, depending on the sample. This leads to uncertainties in the values of rheological parameters. The basic assumptions for measuring the viscosity are (Schramm, 1994):

- laminar flow
- steady state flow
- no slippage
- samples must be homogenous

Due to the nature of the mud sample (e.g., water content, suspension load), it may not be possible to measure viscosity, or at least, the rheometer should be adequately chosen (i.e. geometry, rotation speed, torque sensitivity). The mud may not always behave as a fluid, due to high cohesion or formation of flocs or aggregates, or some problems with sedimentation may occur inside the rheometer. In these cases, the mud viscosity cannot be measured. Measurements of mud viscosity with laboratory rheometers are often only done on the finer fraction (< 100 µm, e.g., Manga et al., 2009) because the majority of rheometers are designed for small samples (e.g., Kopf, 2002). However, several studies have shown that coarser particles in suspension have an effect on the yield stress (Ancey, 2001; Dagois-Bohy et al., 2015; Ovarlez et al., 2015). This also leads to uncertainties in the viscosity of at least one or two orders of magnitude. Samples are often dried after being sieved and later rehydrated. The problem with this procedure is that the sample is normally rehydrated with distilled water and not the original water. As during evaporation not only water but also ions are evaporated, the new rehydrated sample will have a different ionic charge from the original sample, and can thus modify the rheological parameters (Issler, pers. comm.). Another problematic issue is to be sure to add distilled water in the same proportions as for the original sample. This requires that between their sampling and any processing (e.g., water content measurement), the samples were well stored (with respect to temperature and humidity) to prevent evaporation to happen. Indeed, water content strongly affects mud viscosity. For example, Rudolph and Manga (2010) measured a fivefold increase in mud viscosity when the water content decreased from 40% to 33%. All these technical issues occurring during the preparation of the mud sample may affect the measurement of its viscosity, leading to large uncertainties, possibly up to several orders of magnitudes.

Finally, one of the most challenging aspects when determining the rheological parameters to model clastic eruption, is to get a representative sample for the system. Ideally, one should get a sample from the main conduit, during the eruption. However, this may not be possible, and alternative options have to be considered.

As measurements are mostly done on the finest grain fraction, the obtained viscosity can be considered representative of the system if it is mud-dominated. In contrast, if the system is clast-dominated, the viscosity measured in the laboratory will not be representative. For these systems, it is extremely difficult to measure viscosity in the laboratory, as this requires the use of rheometers that could analyse large samples.

### 2.2.3. Density

The densities of each phase should be considered by the model, as both gas and liquid density control the stability of flow patterns and the transition between these patterns. Any change in density of the liquid or gas could potentially trigger a change in the eruption style. The density of solid rock fragments may determine whether they can be carried to the surface during an eruption or not, and cover the range of densities for sedimentary rocks (~ 2200 to 2800 kg $m^{-3}$). Gas density can be derived from the equation for ideal gas and depends on temperature, pressure and molar weight of the gas species. The density varies proportionally with pressure and inversely proportional with temperature. The density of liquid mud is a function of temperature, pressure and water content, and can be calculated using the water content in mass, and the densities of water and clay. The density of mud will range between the density of water (~ 1000 kg $m^{-3}$) and the density of dry clay (~ 2500 kg $m^{-3}$). Both dry clay and water density can vary with temperature, pressure and salinities, but these changes will be small, compared to the variations in gas densities.

One of the cause of overpressure in clastic eruption are the buoyancy forces which are controlled by the density ratio between the ascending fluids and the host rocks. The higher the viscosity contrast, the larger the buoyancy forces and thus the fluid velocities. Densities of host rocks in sedimentary basins can vary between 2200 and 2800 kg $m^{-3}$, which leads to a density ratio from 1.1 to 1.8 between the liquid mud and the host rocks. If the ascending fluids are considered as a single phase, its density depends on the total volume and mass of the fluids (gas and liquid mud) and is controlled by the volume fraction of the gas. If the gas volume fraction is high, the density ratio between the ascending fluid and the host rocks can be large, increasing thus buoyancy forces.

## 2.3. The host rocks

The host rocks play a role in controlling the quantity and velocity of the ascending fluid that depend on buoyant forces, as well as porosity and permeability. Density, porosity and permeability are interconnected parameters that can be reciprocally affected.

### 2.3.1. Density

In clastic eruptions, buried mud and/or sediments ascend due to overpressure at depth which can be caused by density inversion, among other processes. The sediments at depths have a lower density than the shallower overlying rocks which may lead to diapirism (Kopf, 2002). Density inversion may be primary, due to grain density contrast in the deposits, or secondary in origin. Secondary buoyancy can be caused by differential compaction, lateral influx of low-density fluids, variations in sedimentary dynamics, hydrocarbon generation, diagenetic and metamorphic processes or tectonic processes that remove material or otherwise modify the overburden stress field (Mazzini and Etiope, 2017). The density of rocks varies with different lithologies and is influenced by the porosity. It can be calculated as the sum of the density of grains and the density of fluids, contained in pores. During mechanical compaction, the porosity is reduced and the density increases with depth (Athy, 1930). Compaction as a function of burial depths varies greatly within rocks because each primary lithology has a different compaction curve (Baldwin and Butler, 1985). For example, immediately after deposition clay rich sediments have a much greater porosity than sandstones. Thus, a sand bed is denser than a bed of clay or silt, just after deposition. Clay and silt lose their porosity more rapidly with burial than sandstone, and therefore, a bed of clay or silt could be denser than a sand bed at depth. However, when sedimentation rates are high, water may not escape fast enough to reach compaction equilibrium. These sediments may thus have a lower density than the shallower overlying rocks. This may result in mud diapirism that is a common process associated with mud volcanoes and clastic eruptions (Revil, 2002)

### 2.3.2. Porosity and permeability

The porosity is a measure of the void in a rock and is calculated as the ratio of the open space to the total rock volume. It is expressed as a percentage of the total rock which is taken up by pore space. The higher the porosity, the more fluid can be contained in-between grains. The shape of the grains greatly influences the porosity. The grain packing (i.e. the way they are arranged together) also controls the porosity (Beard and Weyl, 1973; Houseknecht, 1987). Well sorted sandstones have a primary porosity around 40-42% just after deposition. Clay-rich sediments have a greater porosity just after deposition, between 60 and 80% (Hantschel and Kauerauf, 2009; Bjørlykke, 2010). Porosity changes with progressive burial due to mechanical and chemical compaction (Bjørlykke, 2010). During mechanical compaction, the solid grains do not change their volume, such that the bulk volume reduction is only equal to porosity loss. Shales, sandstones and carbonates have specific compaction curves and are also controlled by different processes. Both shales and sandstones compact mechanically as a function of effective stress until chemical compaction takes over. Further compaction is mainly a function of temperature and time (Walderhaug, 1996; Bjørkum et al., 1998). The initial mineralogical and textural compositions are of importance for compaction of sandstones and shales. Carbonate sediments can compact chemically at very shallow depth and low temperature. The compaction process is controlled by the interaction between stress and chemical compaction, although the temperature might be less important. The primary content and distribution of aragonite is one of the main factors controlling compaction and rock properties in carbonates (Bjørlykke, 2010). Fluid flow may also increase the permeability and porosity of the host rocks due to fracturing when the pore fluid pressure exceeds the lithostatic pressure (Terzaghi, 1943; Skempton, 1961; Paterson and Wong, 2005). To mimic this effect, the models consider a permeability that is a function of the pore fluid pressure (Lupi et al., 2011; Miller, 2015; Iyer et al., 2017).

The permeability measures the resistance to fluid flow through a rock. It depends on the size of pore spaces in the rocks and the connection between pores. Knowing the pressure difference between the two ends of a horizontal cylinder, the length and cross-section of this cylinder, as well as the viscosity and flow rate of the fluid, it is possible to calculate the permeability using the Darcy equation. Well sorted sandstones may have permeability exceeding 1 Darcy. Compacted clay and silt usually have extremely low permeability values (down to 0.01 nanodarcy), and do not allow the fluid to flow efficiently (Bjørlykke, 2010). For most rocks, the permeability varies with the flow direction. In sedimentary rocks, the permeability is usually higher parallel to the bedding than normal to the bedding. Connected fractures can also greatly increase permeability, especially in rocks that are well-cemented or that have initially extremely low permeabilities. As permeability is controlled by the pore size (i.e. porosity), it reduces with depth in absence of fractures and if the pores are connected.

Porosity and permeability are thus important parameters in models which consider the flow or leakage of a fluid through a porous media, and their variations as a function of temperature and/or depth should be taken into consideration by the model. As both porosity and permeability strongly control oil migration in petroleum systems, these two parameters have been well constrained and compaction and permeability curves are available for different lithologies (Kauerauf and Hantschel, 2009). Such flows and microseepage can be expected in the deeper part of clastic piercements, for example, at the contact with magmatic intrusions where the pore fluids are heated up. These seepages can also be expected in the shallow part of the system, around the main vent. Water and gas, often methane, seepage usually occurs at mud volcanoes and intensifies after each eruption. However, some mud volcanoes, like the Lokbatan mud volcano in Azerbaijan, shows no strong evidence of seepage after large eruptions, suggesting a partial decoupling between the main feeder conduit and the surrounding seepage network (Mazzini and Etiope, 2017).

## 3. Models of clastic eruptions

Multi-phase flow models have been developed over the last decades, initially for industry purposes (Yuster, 1951; Croes et al., 1956; Van Meurs, 1957; Fagin and Stewart Jr, 1966; Yükler et al., 1979; Bethke et al., 1988) and were later adapted to geological systems (e.g., James et al., 2008; Ingebritsen et al., 2010; Lupi et al., 2011). However, up to date, clastic eruptions were only modelled using single-phase flows, to the exception of Sohrabi et al. (2017) who used a two-phase flow models with a formulation of Darcy flow. Nevertheless, the single-phase flow models have sometimes, considered the effect of gas exsolution and expansion on the density and viscosity of the fluid mixture. Two main approaches have been usually applied: either the model considers the flow of fluids through a porous network, and thus employs the Darcy’s law, or the model considers the flow of fluids through a conduit with no porous network, and thus uses the Navier-Stokes equations. Here we present these two formulations.

### 3.1. Darcy flow

The Darcy equation was initially derived experimentally (Darcy, 1856) and describes the flow of a homogenous and isotropic fluid through a porous medium, which has no motion. The equation relates the fluid flux ($q$ in m.s$^{-1}$, discharge per unit area) to the viscosity of the fluid ($\mu$ in Pa·s), the intrinsic permeability of the medium ($\kappa$ in m$^2$) and the pressure gradient vector ($\nabla$p in Pa m$^{-1}$):

$$q = \frac{-\kappa}{\mu}\nabla p \; . \tag{2}$$

The fluid velocity (u) is related to the Darcy flux (q) by the porosity (ϕ), u = q/ϕ.

Models of single-phase fluid flow in a porous medium combine Darcy's law with an equation of state and the conservation of mass (Chen et al., 2006). The mass conservation equation is given by:

$$\frac{\partial(\phi\rho)}{\partial t} = -\nabla.(\rho\mathbf{u}) + s, \tag{3}$$

where $\phi$ is the porosity of the porous medium (the fraction of void available for the fluid), $\rho$ the density of fluid, **u** the superficial Darcy velocity and *s* the external sources and sinks. The momentum conservation in the form of Darcy's law is:

$$\mathbf{u} = -\frac{1}{\mu}\mathbf{k}(\nabla p - \rho\wp\nabla z), \tag{4}$$

where **k** is the absolute permeability tensor of the porous medium, $\mu$ is the fluid viscosity, $\wp$ is the magnitude of the gravitational acceleration and *z* the depth. Substituting eq.(4) in eq.(3) yields:

$$\frac{\partial(\phi\rho)}{\partial t} = \nabla.\left(\frac{\rho}{\mu}\mathbf{k}(\nabla p - \rho\wp\nabla z)\right) + s. \tag{5}$$

An equation of state is expressed in terms of fluid compressibility *cf*:

$$cf = -\frac{1}{V}\frac{\partial V}{\partial p} = \frac{1}{\rho}\frac{\partial \rho}{\partial p}, \tag{6}$$

at a fixed temperature *T*, where *V* stands for the volume occupied by the fluid. Equations (5) and (6) form a closed system for the main unknowns, $p$ and $\rho$.

Darcy's law is only valid for laminar flow through sediments. The dominant parameters for this kind of models are the permeability and porosity of the rocks, and viscosity and density of the fluid.

3.2. Navier-Stokes flow

Another approach is to consider the flow of a fluid in a conduit. In that case, there is no porous "skeleton" through which the fluid is flowing. The fluid is a mixture of liquid mud and gas. For a compressible Newtonian fluid, the conservation of momentum yields:

$$\rho\left(\frac{\partial \mathbf{u}}{\partial t} + \mathbf{u}.\nabla \mathrm{u}\right) = -\nabla p + \nabla.\left(\mu(\nabla \mathbf{u} + (\nabla \mathbf{u})^T)\right) - \frac{2}{3}\mu(\nabla.\mathbf{u})\mathbf{I}) + \mathbf{F}, \tag{7}$$

where **u** is the fluid velocity, p is the fluid pressure $\rho$ is the fluid density and $\mu$ is the fluid dynamic viscosity. The term $\rho\left(\frac{\partial \mathbf{u}}{\partial t} + \mathbf{u}.\nabla \mathrm{u}\right)$ corresponds to the inertial forces, $-\nabla p$ to the pressure forces, $\nabla.\left(\mu(\nabla \mathbf{u} + (\nabla \mathbf{u})^T)\right) - \frac{2}{3}\mu(\nabla.\mathbf{u})\mathbf{I})$ to the viscous forces, and **F** to the external forces applied to the fluid (Batchelor, 1967). The continuity equation gives:

$$\frac{\partial \rho}{\partial t} + \nabla.(\rho \mathbf{u}) = 0. \tag{8}$$

For incompressible flows, the continuity equation can be rewritten as:

$$\nabla.\mathbf{u} = 0, \tag{9}$$

and the term $\frac{2}{3}\mu(\nabla.\mathbf{u})\mathbf{I}$ in eq.(7) can be removed.

When the Reynolds number is small (Re < 1), the inertial forces are small compared to viscous forces and can be neglected in eq. (7), leading to the Stokes equation for incompressible flow:

$$-\nabla p + \mu\nabla^2\mathbf{u} + \mathbf{F} = 0. \tag{10}$$

For models with a Navier-Stokes formulation, density and viscosity of the fluids and of the host rocks, if considered, are key parameters.

## 4. Discussion

The choice between these two formulations depends on the manner fluids are flowing through the host rocks. If the fluids flow through a porous network and the flow is laminar, then a Darcy formulation is more appropriate. For example, around a magmatic intrusion, pore fluids are heated up and flow though the network of pores (Fig. 6). If the fluids flow through a conduit or a pipe and there is no porous network, then the Darcy formulation is incorrect and a Navier-Stokes is preferred. Such flows occur rather in the shallow parts of clastic systems where a vent or cylindrical conduit formed. During clastic eruption, rock fragments and fluids are violently ejected from the conduit, which widens towards the surface (Fig. 6). This suggests that high velocities and turbulent flows are likely to be expected. Consequently, a Darcy formulation to model fluid flow in the main vent during clastic eruption is not adequate as Darcy's law is only valid for laminar flows and restricted to pores. Microseepage may also occur in the upper part of the system, around the main vent and consists in the leakage of liquid or gas through a porous substance. Therefore, a Darcy formulation is more appropriate to model seepage. Modelling the entire clastic system might be challenging because coupling Darcy and Stokes models is problematic as the former only considers pressure gradients while the latter deals with the entire stress tensor. An alternative approach would be to use a Stokes-Brinkman model that is capable of reproducing both Darcy and Stokes flow as end-member cases (Brinkman, 1947; Spaid and Phelan, 1997; Krotkiewski et al., 2011). However, to date no such model has been developed to address fluid flow in clastic eruptions.

The single-phase flow models that have been used for clastic eruptions have the advantage to have a low computational cost and only depends on a few parameters. They easily allow the identification of the first order control of the parameters on the eruption flow rate. Analytical solutions can be used in combination with single-phase models to qualitatively predict the reduction in fluid density due to gas exsolution and expansion at shallow depths (e.g., Rudolph et al., 2011; Collignon et al., 2017). These implementations are based on the equations of state for water, carbon dioxide and methane (e.g., Duan et al., 1992; Duan and Sun, 2003; Spivey et al., 2004; Duan and Mao, 2006). However, these models remain limited and cannot always be valid. First, for turbulent flows, both Darcy and Stokes formulations are not valid, and the full Navier-Stokes equation should rather be considered. Moreover, the analytical implementation considers a fluid mixture density whose value ranges between those for gas and liquid, leading to velocities for the fluid mixture larger than the liquid velocity but smaller than the gas velocity. In two-phase flow systems, the total velocity is defined as a weighted average of the liquid and gas velocities, which depends on both density and viscosity of the gas and liquid. Therefore, depending on how the viscosity of the mixture is computed, single-phase models may underestimate or overestimate the total velocity, with respect to two-phase models. Finally, any variation in gas concentration in single-phase models will only trigger an increase in the flow rate of the eruption but will not be able to reproduce the various eruption styles observed at the surface. To do so, the gas-liquid flow patterns should be considered in the model and investigated, as they are supposed to control the style and dynamics of the eruptions.

Two-phase flow models have not yet been employed to model clastic eruptions partly because these eruptions and the associated geological systems (mud volcanoes and SHHS) have only recently been studied. Therefore, the physical processes associated with these eruptions are less well understood than other well-known geological systems such as magmatic volcanoes or geysers. Further studies of clastic eruptions should look more in details at the work published in the volcanology and geyser literature, as well as in the oil and gas industry, to relate the type of eruptions with the flow patterns. However, most of the studies have focussed on gas-liquid flows and clastic systems might also consider slurry flows with gas and thus have different flow patterns. This will imply different eruption styles, or different transitions between the eruption styles than for gas-liquid flows. Few studies addressed the gas-slurry flow properties (Ding et al., 2016) and further work is thus required. Ding et al., (2016) have recently investigated the flow patterns for gas hydrate slurry flows, and the literature of gas hydrates may provide relevant information for clastic eruptions. Moreover, the rheology of fluids in magmatic systems and geysers is less complex than mud which exhibit a high variability and complex rheology due to its clay content. Finally, the timing of clastic eruptions and the size of associated plumbing systems are not well constrained. While the temporal evolution of clastic eruption associated with SHHS fossil systems is uncertain, the size of the conduit or feeder of modern systems is difficult to constrain on seismic profiles due to the presence of fluids (e.g., Huuse et al., 2010). The monitoring of modern systems, such as the Lusi mud eruption, allows the acquisition of new data to constrain the timing of clastic eruptions and their different phases and types (e.g., Mazzini et al., 2012; Karyono et al., 2017; Mauri et al., 2017). The study of fossil systems brings new constrains on the size of the vent or feeder conduit (e.g., Svensen et al., 2006; Roberts et al., 2010). Future studies should combine the data from modern and fossil systems, as well as the literature from other fields, including volcanology, geysers, industry. This will help to better constrain the dynamics of clastic eruptions as well as their timing and the size of their feeding systems.

The energy of clastic eruptions and the quantity of ejected materials are controlled by the overpressure at depth. The cause of this overpressure may include compaction disequilibrium, primary density inversion or lateral influx of fluids, among other processes. The type of eruption could be related to the liquid-gas flow pattern in the conduit that occurs in the shallow part of the system. One of the most important key parameters in controlling the dynamics of the eruption is the size of this conduit, as it controls the flow patterns in a liquid-gas flow, as well as the Reynolds number for the liquid phase. If the Reynolds number is much smaller than one, viscous forces are dominant while at high Reynolds number (> 3000), the flow is turbulent and thus inertia forces are dominant. Consequently, the conduit size may determine which forces and processes are dominant. Similarly, both density and viscosity of the liquid phase control the flow patterns and are thus key parameters. We stress that both the size of the conduit and the properties of the fluid should be constrained to identify the dominant forces and physical processes and choose the appropriate model.

## 5. Conclusion

Here we summarise the principal components that should ideally be considered when modelling fluid flow in clastic erupting systems: the geometry of the plumbing system, the transported material and its properties, and the host rocks. Each of these components affects the main processes and parameters controlling the dynamics of the eruptions. The challenges and limitations associated with the characterisation and quantification of these parameters and processes are also presented. We suggest that similarly to magmatic systems, the liquid-gas flow pattern could control the type of eruption. Explosive eruptions characterised by large muddy bubbles could be explained in term of slug or churn flows, while annular flows could be expected for the more effusive eruptions characterised by enhanced degassing. The slow extrusion of mud with little bubbling activity, observed at mud volcanoes, could be related to a bubbly flow in the conduit. We suggest that the occurrence of slug flow in clastic systems may not occur, depending on the viscosity of liquid mud. Moreover, we propose, based on the gas volume fraction, values for the depths at which transitions between the different flow patterns could occur in the conduit for a given methane or carbon dioxide concentration. However, these conclusions remain highly speculative and have not yet been supported by experimental, numerical nor field data for clastic eruptions and therefore further work is required.

Due to the complexity of the processes and the difficulties to characterise them, simplification are required to model clastic eruptions. Up to date, only single-phase flow models have been employed and we present here the two main formulations, used to model fluid flows in clastic eruption: Darcy and Navier-Stokes, and their controlling parameters. The choice between a Darcy and Navier-Stokes formulation depends on the manner fluid flows through the host rocks, as well as the flow regime. If the fluids migrate through a porous network, a Darcy formulation is preferred and porosity and permeability are key parameters. If there is no porous network, a Navier-Stokes formulation is more appropriated and the viscosity and density of the fluid and the host rocks are key parameters. Although single-phase models allow the identification of first order controls of various parameters on the eruption flow rate, they are limited and do not allow an accurate quantification of these parameters. These models also do not reproduce the different types of eruptions. Therefore, further work is needed on clastic systems and the literature from other fields, such as volcanology, oil and gas or nuclear industry should be considered to better constrain the dynamics of the eruptions as well as their temporal and spatial resolution.

Acknowledgments:

The work was funded by the European Research Council under the European Union's Seventh Framework Programme Grant agreement n° 308126 (LUSI LAB project, PI A. Mazzini). We acknowledge the support from the Research Council of Norway through its Centres of Excellence funding scheme, Project Number 223272. Matteo Lupi acknowledge the AP Energy Grant, project number PYAPP2_166900. Christophe Ancey, Dieter Issler, Marie Violay and Abigail L. Bull are thanked for fruitful discussions. The authors also thank the Editor and two anonymous Reviewers.

References:

Aliyev, A., Guliyev, I., and Belov, I. S., 2002, Catalogue of Recorded Eruptions of Mud Volcanoes of Azerbaijan, Baku, Nafta Press.

Ancey, C., 2001, Role of lubricated contacts in concentrated polydisperse suspensions: Journal of Rheology, v. 45, no. 6, p. 1421-1439.

Ancey, C., and Jorrot, H., 2001, Yield stress for particle suspensions within a clay dispersion: Journal of Rheology, v. 45, no. 2, p. 297-319.

Aoki, Y., and Sidiq, T. P., 2014, Ground deformation associated with the eruption of Lumpur Sidoarjo mud volcano, east Java, Indonesia: Journal of Volcanology and Geothermal Research, v. 278-279, p. 96-102.

Athy, L. F., 1930, Density, porosity and compaction of sedimentary rock: AAPG Bulletin, v. 14, p. 1-24.

Baldwin, B., and Butler, C. O., 1985, Compaction Curves: AAPG Bulletin, v. 69, no. 4, p. 622-626.

Barnea, D., 1987, A unified model for predicting flow-pattern transitions for the whole range of pipe inclinations: International Journal of Multiphase Flow, v. 13, no. 1, p. 1-12.

Batchelor, G. K., 1967, An Introduction to Fluid Dynamics, Cambridge University Press.

Beard, D. C., and Weyl, P. K., 1973, Influence of Texture on Porosity and Permeability of Unconsolidated Sand: AAPG Bulletin, v. 57, no. 2, p. 349-369.

Bell, B., and Butcher, H., 2002, On the emplacement of sill complexes: evidence from the Faroe-Shetland Basin, *in* Jolley, D. W., and Bell, B. R., eds., The North Atlantic Igneous Province: Stratigraphy, Tectonic, Volcanic and Magmatic Processes, Volume 197, Geological Society, London, Special Publication, p. 307-329.

Berlamont, J., Ockenden, M., Toorman, E. A., and Winterwerp, J., 1993, The characterisation of cohesive sediment properties: Coastal Engineering, v. 21.

Berndt, C., Hensen, C., Mortera-Gutierrez, C., Sarkar, S., Geilert, S., Schmidt, M., Liebetrau, V., Kipfer, R., Scholz, F., Doll, M., Muff, S., Karstens, J., Planke, S., Petersen, S., Böttner, C., Chi, W.-C., Moser, M., Behrendt, R., Fiskal, A., Lever, M. A., Su, C.-C., Deng, L., Brennwald, M. S., and Lizarralde, D., 2016, Rifting under steam - How rift magmatism triggers methane venting from sedimentary basins Geology

Bethke, C. M., Altaner, S. P., Harrison, W. J., and Upson, C., 1988, Supercomputer Analysis of Sedimentary Basins: Science v. 239, p. 261-267.

Bjørkum, P. A., Oelkers, E. H., Nadeau, P. H., Walderhaug, O., and Murphy, W. M., 1998, Porosity Prediction in Quartzose Sandstones as a function of Time, Temperature, Depth, Stylolite Frequency, and Hydrocarbon Saturation: AAPG Bulletin, v. 82, no. 4, p. 637-648.

Bjørlykke, K., 2010, Petroleum Geoscience: From Sedimentary Environments to Rock Physics, Heidelberg, Springer.

Bonadonna, C., and Costa, A., 2013, Plume height, volume, and classification of explosive volcanic eruption based on the Weibull function: Bulletin of Volcanology, v. 75, no. 8.

Bonini, M., 2012, Mud volcanoes: Indicators of stress orientation and tectonic controls: Earth-Science Reviews, v. 115, p. 121-152.

Brennen, C. E., 2005, Fundamentals of Multiphase Flows, Cambridge, Cambridge University Press.

Brinkman, H. C., 1947, A calculation of the viscous force exerted by a flowing fluid on a dense swarm of particles: Appl. Sci. Res. , v. 1, no. 1, p. 27-34.

Brodkey, R. S., 1967, The phenomena of Fluid Motions, Addison-Wesley Press.

Campbell, K. A., 2006, Hydrocarbon seep and hydrothermal vent paleoenvironments and paleontology: Past developments and future research direction: Palaeogeography, Palaeoclimatology, Palaeoecology, v. 232, p. 362-407.

Campos, M., Takahashi, T., Ashikawa, F., Simões, S., Stender, A., and Meien, O., 2015, Advanced Anti-slug Control for Offshore Production Plants: IFAC-PapersOnLine, v. 48, no. 6, p. 83-88.

Chapoy, A., Mohammadi, A. H., Chareton, A., Tohidi, B., and Richon, D., 2004, Measurements and Modeling of Gas Solubility and Literature Review of the Properties for the Carbon Dioxide-Water System: Industrial and Engineering Chemistry Research, v. 43, p. 1794-1802.

Cheng, H., Hills, J. H., and Azzopardi, B. J., 1998, A study of the bubble-to-slug transition in vertical gas-liquid flow in columns of different diameter: International Journal of Multiphase Flow, v. 24, p. 431-452.

Cheng, H., Hills, J. H., and Azzopardi, B. J., 2002, Effect of initial bubble size on flow pattern transition in a 28.9 mm diameter column: International Journal of Multiphase Flow, v. 28, p. 1047-1062.

Cioncolini, A., and Thome, J. R., 2012, Void fraction prediction in annular two-phase flow: International Journal of Multiphase Flow, v. 43, p. 72-84.

Ciotoli, G., Etiope, G., Marra, F., Florindo, F., Giraudi, C., and Ruggiero, L., 2016, Tiber delta $CO_2$-$CH_4$ degassing: a possible hybrid, tectonically active Sediment-Hosted Geothermal System near Rome: Journal of Geophysical Research, v. 121, no. 1, p. 48-69.

Clift, R., Grace, J. R., and Weber, M. E., 1978, Bubbles, Drops and Particles, San Diego, Academic, 380 p.

Collignon, M., Schmid, D.W., Gallerne, C., Lupi, M., and Mazzini, A., 2017, Modelling fluid flow in clastic eruptions: Application to the Lusi mud eruption: Marine and Petroleum geology, this issue, 18p.

Coussot, P., 1994, Steady, laminar flow of concentrated mud suspensions in open channel: Journal of Hydraulic Research, v. 32, p. 535-559.

Coussot, P., 1995, Structural Similarity and Transition from Newtonian to Non-Newtonian Clay-Water Suspensions: Physical Review Letters v. 74, no. 20, p. 3971-3974.

Coussot, P., and Boyer, S., 1995, Determination of yield stress fluid behaviour from inclined plane test: Rheologica Acta, v. 34, p. 534-543.

Croes, G. A., Geertsma, J., and Schwarz, N., 1956, Theory of dimensionally scaled models of Petroleum Reservoirs: Transaction of AIME v. 207, p. 118.

Dagois-Bohy, S., Hormozi, S., Guazzelli, E., and Pouliquen, O., 2015, Rheology of dense suspensions of non-colloidal spheres in yield-stress fluids: Journal of Fluid Mechanics, v. 776, p. 1-11.

Darcy, H., 1856, Les Fontaines Publiques de la ville de Dijon, Paris, Victor Dalmand.

Davies, R. J., Mathias, S. A., Swarbrick, R., and al., e., 2011, Probabilistic longevity estimate for the LUSI mud volcano, East Java: Journal of the Geological Society v. 168, p. 517-523.

Deville, E., and Guerlais, S.-H., 2009, Cyclic activity of mud volcanoes: Evidences from Trinidad (SE Caribbean): Marine and Petroleum Geology, v. 26, p. 1681-1691.

Diamond, L., and Akinfiev, N. N., 2003, Solubility of CO2 in water from -1.5 to 100ºC and from 0.1 to 100 MPa: evaluation of literature data and thermodynamic modelling: Fluid Phase Equilibria v. 208, p. 265-290.

Dimitrov, L. I., 2002, Mud volcanoes - the most important pathway for degassing deeply buried sediments: Earth-Science Reviews, v. 59, p. 49-76.

Ding, L., Shi, B., Lv, X., Liu, Y., Wu, H., Wang, W., and Gong, J., 2016, Investigation of natural gas hydrate slurry flow properties and flow patterns using a high pressure flow loop: Chemical Engineering Science, v. 146, p. 199-206.

Duan, Z., and Mao, S., 2006, A thermodynamic model for calculating methane solubility, density and gas phase composition of methane-bearing aqueous fluids from 273 to 523K and from 1 to 2000 bar: Geochimica et Cosmochimica Acta, v. 70, p. 3369-3386.

Duan, Z., Møller, N., and Weare, J. H., 1992, An equation of state for the CH4-CO2-H20 system: I. Pure systems from 0 to 1000ºC and 0 to 8000 bar Geochimica et Cosmochimica Acta, v. 56, p. 2605-2617.

Duan, Z., and Sun, R., 2003, An improved model calculating CO2 solubility in pure water and aqueous NaCl solutions from 273 to 533 K and from 0 to 2000 bar Chemical Geology, v. 193, p. 257-271.

Etiope, G., 2015, Natural Gas Seepage, Switzerland, Springer 193pp p.:

Etiope, G., and Milkov, A. V., 2004, A new estimate of global methane flux from onshore and shallow submarine mud volcanoes to the atmosphere Environmental Geology, v. 46, no. 8, p. 997-1002.

Fagin, R. G., and Stewart Jr, C. H., 1966, A new approach to the two-dimensional multiphase reservoir simulator: Society of Petroleum Engineers Journal, v. 6, p. 175-182.

Fowler, S. R., Mildenhall, J., Zalova, S., Riley, G., Elsley, G., Desplanques, A., and Guliyev, F., 2000, Mud volcanoes and structural development on Shah Deniz: Journal of Petroleum Science and Engineering v. 28, p. 189-206.

Fukushima, Y., Cayol, V., and Durand, P., 2005, Finding realistic dike models from interferometric syntheric aperture radar data: the February 2000 eruption at Piton de la Fournaise.: Journal of Geophysical Research, v. 110.

Fukushima, Y., Mori, J., Hashimoto, M., and Kano, Y., 2009, Subsidence associated with the LUSI mud eruption, East Java, investigated by SAR interferometry: Marine and Petroleum Geology, v. 26, p. 1740-1750.

Gisler, G., 2009, Simulations of the explosive eruption of superheated fluids through deformable media: Marine and Petroleum Geology, v. 26, p. 1888-1895.

Graue, K., 2000, Mud volcanoes in deepwater in Nigeria: Marine and Petroleum Geology, v. 17, p. 959-974.

Guet, S., Ooms, G., and Oliemans, R. V. A., 2002, Influence of bubble size on the transition from low-Re bubbly flow to slug flow in a vertical pipe: Exp. Therm. Fluid Sci. , v. 26, p. 635-641.

Guliev, I. S., 1992, A review of mud volcanism. .

Guo, G.-J., and Rodger, P. M., 2013, Solubility of Aqueous Methane under Metastable Conditions: Implications for Gas Hydrate Nucleation: Journal of Physical Chemistry, v. 117, no. 21, p. 6498-6504.

Hantschel, T., and Kauerauf, A. I., 2009, Fundamentals of Basin and Petroleum Systems Modeling Heidelberg, Springer

Hewhall, C. G., and Self, S., 1982, The volcanic explosivity index (VEI) an estimate of explosive magnitude for historical volcanism: Journal of Geophysical Research: Oceans, v. 87, no. C2, p. 1231-1238.

Hewitt, G., 1999, Introduction and Basic Models, *in* Kandlikar, S. G., Shoji, M., and Dhir, V. K., eds., Handbook of Phase Change, Boiling and Condensation: Philadelphia, Taylor and Francis, p. 197-203.

Houseknecht, D. W., 1987, Assessing the Relative Importance of Compaction Processes and Cementation to Reduction of Porosity in Sandstones: AAPG Bulletin, v. 71, no. 6, p. 633-642.

Huuse, M., Jackson, C. A.-L., Van Rensbergen, P., Davies, R. J., Flemings, P. B., and Dixon, R. J., 2010, Subsurface sediment remobilization and fluid flow in sedimentary basins: an overview: Basin Research, v. 22, p. 342-360.

Ingebritsen, S. E., Geiger, S., Hurwitz, S., and Driesner, T., 2010, Numerical simulation of magmatic hydrothermal systems.: Reviews of Geophysics, v. 48, p. 33.

Istadi, B., Pramono, G. H., Sumintadireja, P., and Alam, S., 2009, Modeling study of growth and potential geohazard for LUSI mud volcano: Marine and Petroleum Geology, v. 26, p. 1724-1739.

Iyer, K., Rüpke, L., and Galerne, C. Y., 2013, Modeling fluid flow in sedimentary basins with sill intrusions: Implications for hydrothermal venting and climate change: Geochemistry, Geophysics, Geosystems, v. 14, no. 12, p. 5244-5262.

Iyer, K., Schmid, D. W., Planke, S., and Millett, J., 2017, Modelling hydrothermal venting in volcanic sedimentary basins: Impact on hydrocarbon maturation and paleoclimate: Earth and Planetary Science Letters, v. 467, p. 30-42.

James, M. R., Lane, S. J., Chouet, B., and Gilbert, J. S., 2004, Pressure changes associated with the ascent and bursting of gas slugs in liquid-filled vertical and inclined conduits.: Journal of Volcanology and Geothermal Research, v. 129, p. 61-82.

James, M. R., Lane, S. J., and Corder, S. B., 2008, Modelling the rapid near-surface expansion of gas slugs in low viscosity magma, *in* Lane, S. J., and Gilbert, J. S., eds., Fluid motion in volcanic conduits: A source of seismic and acoustic signals: London, Geological Society, Special Publications, p. 147-167.

James, M. R., Lane, S. J., Wilson, L., and Corder, S. B., 2009, Degassing at low magma-viscosity volcanoes: Quantifying the transition between passive bubble-burst and Strombolian eruption: Journal of Volcanology and Geothermal Research, v. 180, p. 81-88.

James, M. R., Llewellin, E. W., and Lane, S. J., 2011, Comments on "It takes three to tango: 2. Bubble dynamics in basaltic volcanoes and ramification for modelling normal Strombolian activity" by Suckale, J. et al.: Journal of Geophysical Research, v. 113.

Jamtveit, B., Svensen, H., Podladchikov, Y. Y., and Planke, S., 2004, Hydrothermal vent complexes associated with sill intrusions in sedimentary basins, *in* Breitkreuz, C., and Petford, N., eds., Physical Geology of High-Level Magmatic Systems, Volume 234: London, Geological Society, London, Special Publication, p. 233-241.

Jaupart, C., and Vergniolle, S., 1989, The generation and collapse of a foam layer at the roof of a basaltic magma chamber Journal of Fluid Mechanics, v. 203, p. 347-380.

Judd, A. G., Hovland, M., Dimitrov, L. I., Garcia Gil, S., and Jukes, V., 2002, The geological methane budget at Continental Margins and its influence on climate change Geofluids v. 2, no. 2, p. 109-126.

Karyono, K., Obermann, A., Lupi, M., Masturyono, M., Hadi, S., Syafri, I., Abdurrokhim, A., and Mazzini, A., 2017, Lusi, a clastic-dominated geysering system in Indonesia recently explored by surface and subsurface observations: Terra Nova, v. 29, p. 13-19.

Kauerauf, A. I., and Hantschel, T., 2009, Fundamentals of Basin and Petroleum Systems Modeling, Heidelberg, Springer.

Keating, G., and Valentine, G., 2008, Shallow plumbing systems for small-volume basaltic volcanoes: Bulletins of Volcanology, v. 70, p. 563-582.

Kholodov, V. N., 2002, Mud Volcanoes, Their Distribution Regularities and Genesis Communication 1. Mud Volcanic Provinces and Morphology of Mud Volcanoes: Lithology and Mineral Resources, v. 37 no. 3, p. 197-209.

Kopf, A. J., 2002, Significance of Mud Volcanism Reviews of Geophysics, v. 40, no. 2, p. 1-52.

Kopf, A. J., 2003, Global methane emission throuh mud volcanoes and its past and present impact of the Earth's climate: International Journal of Earth Sciences, v. 92, p. 806-816.

Kopf, A. J., and Behrmann, J. H., 2000, Extrusion dynamics of mud volcanoes on the Mediterranean Ridge accretionary complex, *in* Vendeville, B., Mart, Y., and Vigneresse, J.-L., eds., From the Arctic to the Mediterranean: Salt, Shale, and Igneous Diapirs in and Around Europe, Volume 174, Geological Society Special Publications, p. 169-204.

Krotkiewski, M., Ligaarden, I. S., Lie, K.-A., and Schmid, D. W., 2011, On the Importance of the Stokes-Brinkman Equations for Computing Effective Permeability in Karst Reservoirs: Communications in Computational Physics v. 10, no. 5, p. 1315-1332.

Kvenvolden, K. A., and Rogers, B. W., 2005, Gaia's breath - global methane exhalations: Marine and Petroleum Geology, v. 22, p. 579-590.

Lance, S., Henry, P., Le Pichon, X., Lallemant, S., Chamley, H., Rostek, F., Faugères, J. C., Gonthier, E., and Olu, K., 1998, Submersible study of mud volcanoes seaward of the Barbados accretionary wedge: sedimentology, structure and rheology: 1998, v. 145, p. 255-292.

Lecampion, B., and Garagash, D. I., 2014, Confined flow of suspensions modelled by a frictional rheology: Journal of Fluid Mechanics, v. 759, p. 197-235.

Lee, G. H., Kwon, Y. I., Yoon, C. S., Kim, H. J., and Yoo, H. S., 2006, Igneous complexes in the eastern Northern South Yellow Sea Basin and their implications for hydrocarbon systems: Marine and Petroleum Geology, v. 23, no. 6, p. 631-645.

Locat, J., and Demers, D., 1988, Viscosity, yield stress, remolded strength, and liquidity index relationships for sensitive clays Canadian Geotechnical Journal, v. 25, p. 799-806.

Lupi, M., Geiger, S., and Graham, C. M., 2011, Numerical simulations of seismicity-induced fluid flow in the Tjörnes Fracture Zone, Iceland: Journal of Geophysical Research, v. 116, no. B7, p. 17.

Lyons, J. J., Waite, G. P., Rose, W. I., and Chigna, G., 2010, Patterns in open vent, strombolian behavior at Fuego volcano, Guatemala: Bulletins of Volcanology, v. 72, p. 1-15.

Mader, H. M., Llewellin, E. W., and Mueller, S. P., 2013, The rheology of two-phase magmas: a review and analysis: Jounal of Volcanology and Geothermal Research, v. 257, p. 135-158.

Major, J. J., and Pierson, T. C., 1992, Debris Flow Rheology: Experimental Analysis of Fine-Grained Slurries: Water Resources Research, v. 28, no. 3, p. 841-857.

Manga, M., Brumm, M., and Rudolph, M. L., 2009, Earthquake triggering of mud volcanoes Marine and Petroleum Geology, v. 26, p. 1785-1798.

Mao, S., Zhang, Z., Li, Y., and Liu, N., 2013, An improved model for calculating CO2 solubility in aqueous NaCl solutions and the applications to CO2-H2O-NaCl fluid inclusions: Chemical Geology, v. 347, p. 43-58.

Mauri, G., Husein, A., Mazzini, A., Irawan, D., Sohrabi, R., Hadi, S., Prasetyo, H., and Miller, S. A., 2017, Insights on the structure of Lusi mud edifice from land gravity data: Marine and Petroleum Geology, v. in press.

Mazzini, A., 2009, Mud volcanism: Processes and implications: Marine and Petroleum Geology, v. 26, p. 1677-1680.

Mazzini, A., and Etiope, G., 2017, Mud volcanism: An updated review: Earth-Science Reviews, v. 168, p. 81-112.

Mazzini, A., Etiope, G., and Svensen, H., 2012, A new hydrothermal scenario for the 2006 Lusi eruption, Indonesia. Insights from gas geochemistry Earth and Planetary Science Letters, v. 317-318, p. 305-318.

Mazzini, A., Nermoen, A., Krotkiewski, M., Podladchikov, Y., Planke, S., and Svensen, H., 2009, Strike-slip faulting as a trigger mechanism for overpressure release through piercement structures. Implications for the Lusi mud volcano, Indonesia: Marine and Petroleum Geology, p. 1-15.

McNutt, S. R., 1996, Seismic Monitoring and Eruption Forecasting of volcanoes: a review of the State-of-the-Art and Case Histories *in* Scarpa, and Tilling, eds., Monitoring and Mitigation of Volcano Hazards, Springer, p. 99-146.

Mewis, J., and Wagner, N., 2009, Thixotropy: Advances in Colloid and Interface Science, p. 214-227.

Milkov, A. V., 2000, Worldwide distribution of submarine mud volcanoes and associated gas hydrates: Marine Geology, v. 167, p. 29-42.

Milkov, A. V., Sassen, R., Apanasovich, T. V., and Dadashev, F. G., 2003, Global gas flux from mud volcanoes: a significant source of fossil methane in the atmosphere and the ocean Geophysical Research Letters, v. 30, no. 2, p. 9pp.

Miller, S. A., 2015, Modeling enhanced geothermal systems and the essential nature of large-scale changes in permeability at the onset of slip: Geofluids, v. 15, p. 338-349.

Mogi, K., 1958, Relations between the Eruptions of Various Volcanoes and the Deformations of the Ground Surfaces around them: Bulletin of the Earthquake research institute, v. 36, p. 99-134.

Mordret, A., Rivet, D., Landès, M., and Shapiro, N. M., 2015, Three-dimensional shear velocity anisotropic model of Piton de la Fournaise Volcano (La Réunion Island) from ambient seismic noise: Journal of Geophysical Research, Solid Earth, v. 120, p. 406-427.

Moss, J. L., and Cartwright, J., 2010, 3D seismic expression of km-scale fluid escape pipes from offshore Namibia: Basin Research, v. 22, p. 481-501.

Nermoen, A., Galland, O., Jettestuen, E., Fristad, K., Podladchikov, Y., Svensen, H., and Malthe-Sørenssen, A., 2010, Experimental and analytical modeling of piercement structures Journal of Geophysical Research, v. 115, p. 15.

Obermann, A., Lupi, M., Mordret, A., Jakobsdóttir, S. S., and Miller, S. A., 2016, 3D ambient noise Rayleigh wave tomography of Snæfellsjökull volcano, Iceland: Journal of Volcanology and Geothermal Research, v. 317, p. 42-52.

Ohnuki, A., and Akimoto, H., 2000, Experimental study on transition of flow pattern and phase distribution in upward air-water two-phase flow along a large vertical pipe: International Journal of Multiphase Flow, v. 26, p. 367-386.

Omebere-Iyari, N. K., Azzopardi, B. J., and Ladam, Y., 2007, Two-phase flow patterns in large diameter vertical pipes at high pressures: AIChE Journal, v. 53, p. 2493-2504.

Omebere-Iyari, N. K., Azzopardi, B. J., and Ladam, Y., 2008, The characteristics of gas/liquid flow in large risers at high pressures: International Journal of Multiphase Flow v. 34, p. 461-476.

Ovarlez, G., Mahaut, F., Deboeuf, N., Lenoir, S., Hormozi, S., and Chateau, X., 2015, Flows of suspensions of particles in yield stress fluids: Journal of Rheology, v. 59.

Parfitt, E. A., 2004, A discussion on the mechanisms of explosive basaltic eruptions: Journal of Volcanology and Geothermal Research, v. 134, p. 77-107.

Paterson, M. S., and Wong, T.-F., 2005, Experimental Rock Deformation- The Brittle Field Berlin, Springer, 346 p.:

Pickering, P., Hewitt, G., Watson, M., and Hale, C., 2001, The prediction of flows in production risers - truth & myth ?, IIR Conference

Pioli, L., Bonadonna, C., Azzorpardi, B. J., Phillips, J. C., and Ripepe, M., 2012, Experimental constraints on the outgassing dynamics of basaltic magmas: Journal of Geophysical Research, v. 117, no. B03204, p. 1-17.

Planke, S., Rasmussen, T., Rey, S. S., and Myklebust, R., 2005, Seismic characteristics and distribution of volcanic intrusions and hydrothermal vent complexes in the Vøring and Møre basins, *in* Doré, A. G., and Vining, B. A., eds., Petroleum Geology: North-West Europe and Global Perspectives- Proceedings of the 6th Petroleum Geology Conference: London, The Geological Society p. 833-844.

Planke, S., Svensen, H., Hovland, M., Banks, D., and Jamtveit, B., 2003, Mud and fluid migration in active mud volcanoes in Azerbaijan: Geo-Mar Lett, v. 23, p. 258-268.

Qin, J., Rosenbauer, R. J., and Duan, Z., 2008, Experimental Measurements of Vapor-Liquid Equilibria of the H2O + CO2 + CH4 Ternary system: Journal of Chemical and Engineering Data, v. 53, p. 1246-1249.

Revil, A., 2002, Genesis of mud volcanoes in sedimentary basins: A solitary wave-based mechanism.: Geophysical Research Letters, v. 29, no. 12.

Roberts, K. S., Davies, R. J., and Stewart, S. A., 2010, Structure of exhumed mud volcano feeder complexes, Azerbaijan: Basin Research, v. 22, p. 439-451.

Rudolph, M. L., Karlstrom, L., and Manga, M., 2011, A prediction of the longevity of the Lusi mud eruption, Indonesia: Earth and Planetary Science Letters, v. 308, p. 124-130.

Rudolph, M. L., and Manga, M., 2010, Mud volcano response to the 4 April 2010 El Mayor-Cucapah earthquake: Journal of Geophysical Research, v. 115, p. 14.

Ryan, M. P., 1988, The mechanics and three-dimensional internal structure of active magmatic systems: Kilauea volcano, Hawaii: Journal of Geophysical Research, v. 93, p. 4213-4248.

Schnyukov, E. F., Sobolevskiy, Y. V., Gnatenko, G. I., Naumenko, P. I., and Kutniy, V. A., 1986, Mud Volcanoes of Kerch-Taman Region Kiev, Naukova Dumka.

Schramm, G., 1994, A Practical Approach to Rheology and Rheometry.

Shirzae, M., Rudolph, M. L., and Manga, M., 2015, Deep and shallow sources for the Lusi mud eruption revealed by surface deformation: Geophysical Research Letters, v. 42, no. 13, p. 5274-5281.

Sigurdsson, H., Houghton, B., Rymer, H., Stix, J., and McNutt, S., 1999, Encyclopedia of Volcanoes, Elsevier.

Skempton, A. W., 1961, Effective stress in soil, concrete and rocks Pore Pressure and Suction in Soils: London, Butterworths, p. 4-16.

Sohrabi, R., Jansen, G., Malvoisin, B., Miller, S.A., 2017, Numerical modeling of the Lusi hydrothermal system: Initial results and future challenges, this issue, 10 p.

Spaid, M. A. A., and Phelan, F. R., 1997, Lattice Boltzmann methods for modeling microscale flow in fibrous porous media: Physics of Fluids v. 9, p. 2468-2474.

Spivey, J. P., Mccain, W. D., and North, R., 2004, Estimating density formation volume factor, compressibility, methane solubility, and viscosity for oilfield brines at temperatures from 0 to 275ºC, pressures to 200 MPa, and salinities to 5.7 mole/kg: Journal of Canadian Petroleum Technologies, v. 43, no. 7, p. 52-60.

Stickel, J. J., Phillips, R. J., and Powell, R. L., 2007, Application of a constitutive model for particulate suspensions: Time-dependent viscometric flows: Journal of Rheology, v. 51, no. 6.

Storkaas, E., and Skogestad, S., 2007, Controllability analysis of two-phase pipeline-riser systems at riser slugging conditions: Control Engineering Practice, v. 15, p. 567-581.

Svensen, H., Hammer, Ø., Mazzini, A., Onderdonk, N., Polteau, S., Planke, S., and Podladchikov, Y., 2009a, Dynamics of hydrothermal seeps from the Salton Sea geothermal system (California, USA) constrained by temperature monitoring and time series analysis.: Journal of Geophysical Research Solid Earth, v. 114.

Svensen, H., Jamtveit, B., Planke, S., and Chevallier, L., 2006, Structure and evolution of hydrothermal vent complexes in the Karoo Basin, South Africa: Journal of the Geological Society, London, v. 163, p. 671-682.

Svensen, H., Planke, S., Chevallier, L., Malthe-Sørenssen, A., Corfu, F., and Jamtveit, B., 2007, Hydrothermal venting of greenhouse gases triggering Early Jurassic global warming: Earth and Planetary Science Letters, v. 256, p. 554-566.

Svensen, H., Planke, S., Jamtveit, B., and Pedersen, T., 2003, Seep carbonate formation controlled by hydrothermal vent complexes: a case study from the Vøring Basin, the Norwegian Sea: Geo-Mar LEtt., v. 23, p. 351-358.

Svensen, H., Planke, S., Malthe-Sørenssen, A., Jamtveit, B., Myklebust, R., Eidem, T. R., and Rey, S. S., 2004, Release of methane from a volcanic basin as a mechanism for initial Eocene global warming: Nature, v. 429, p. 542-545.

Svensen, H., Planke, S., Polozov, A. G., Schmidbauer, N., Corfu, F., Podladchikov, Y., and Jamtveit, B., 2009b, Siberian gas venting and the end-Permian environmental crisis: Earth and Planetary Science Letters, v. 277, p. 490-500.

Taha, T., and Cui, Z. F., 2006, CFD modelling of slug flow in vertical tubes: Chemical Engineering Science v. 61, p. 676-687.

Taitel, Y., Bornea, D., and Dukler, A. E., 1980, Modelling flow Pattern Transitions for Steady Upward Gas-Liquid Flow in Vertical Tubes: AIChE Journal, v. 26, no. 3, p. 345-354.

Terzaghi, K., 1943, Theoritical Soil Mechanics, New York, John Wiley and Sons.

Thordarson, T., and Larsen, G., 2007, Volcanism in Iceland in historical time: Volcano types, eruption styles and eruptive history: Journal of Geodynamics, v. 43, no. 1, p. 118-152.

Toma, P., Vargas, E., and Kuru, E., 2006, Prediction of Slug-to-Annular Flow Pattern Transition (SAT) for Reducing the Risk of Gas Lift Instabilities and Effective Gas/Liquid Transport From Low-Pressure Reservoirs, *in* Engineers, S. o. P., ed., SPE Gas Technology Symposium Volume SPE 100615: Calgary, Alberta, Canada, p. 1-10.

Toorman, E. A., 1994, An analytical solution for the velocity and shear rate distribution of non-ideal Bingham fluids in concentric cylinder viscometers: Rheologica Acta, v. 33, p. 193-202.

Toorman, E. A., 1997, Modelling the thixotropic behaviour of dense cohesive sediment suspensions: Rheologica Acta, v. 36, p. 56-65.

Van Meurs, P., 1957, The use of transparent three-dimensional models for studying the mechanism of flow processes in oil reservoirs Society of Petroleum Engineers Journal, v. 210, p. 295-301.

Vergniolle, S., and Jaupart, C., 1986, Separated two-phase flow and basaltic eruptions: Journal of Geophysical Research, v. 91, no. B12, p. 12842-12860.

Walderhaug, O., 1996, Kinetic modelling of quartz cementation and porosity loss in deeply buried sandstone reservoir.: AAPG Bulletin, v. 80, p. 731-745.

Walker, G. P. L., 1973, Explosive volcanic eruptions - a new classification scheme: Geologische Rundschau, v. 62, no. 2, p. 431-446.

Wallis, G. B., 1969, One-dimensional two-phase flow McGraw-Hill Book Co.

Weisman, J., 1983, Two-phase flow patterns, *in* Cheremisinoff, N. P., and Gupta, R., eds., Handbook of Fluids in Motions, Ann Arbor Science Publ. , p. 409-425.

Welhan, J. A., and Lupton, J. E., 1987, Light-hydrocarbon gases in Guaymas Basin hydrothermal fluids - thermogenic versus abiogenic origin: AAPG Bulletin, v. 71, p. 215-223.

Wignall, P. B., 2001, Large igneous provinces and mass extinctions: Earth-Science Reviews, v. 53, p. 1-33.

Wilson, L., Sparks, R. S., and Walker, G. P. L., 1980, Explosive volcanic eruptions: -IV the control of magma properties and conduit geometry on eruption column behaviour: Geophysical Journal International, v. 63, no. 1, p. 117-148.

Wörner, 2003, A Compact Introduction to the Numerical Modeling of Multiphase Flows, Karlsruhe, Forschungszentrum Karlsruhe GmbH, 47 p.:

-, 2012, Numerical modeling of multiphase flows in microfluidics and micro process engineering: a review of methods and applications: Microfluid Nanofluid, v. 12, p. 841-886.

Yamamoto, S., Alcauskas, J. B., and Crozier, T. E., 1976, Solubility of methane in distilled water and seawater: Journal of Chemical and Engineering Data, v. 21, no. 1, p. 78-80.

Yamato, P., Duretz, T., May, D. A., and Tartèse, R., 2015, Quantifying magma segregation in dykes: Tectonophysics, v. 660, p. 132-147.

Yükler, M. A., Cornford, C., and Welte, D., 1979, Simulation of geologic, hydrodynamic and thermodynamic development of a sediment basin - a quantitative approach: Initial reports of the Deep Sea Drilling Project v. 38, p. 761-771.

Yuster, S. T., 1951, Theoritical considerations of multiphase flow in idealized capillary systems: Proceedings of the 3rd World Petroleum Congress.

Zoporowski, A., and Miller, S. A., 2009, Modelling eruption cycles and decay of mud volcanoes: Marine and Petroleum Geology, v. 26, p. 1879-1887.

**Figure captions:**

**Fig. 1**: Examples of modern and fossil clastic piercements: a) Lokbatan mud volcano, Azerbaijan, eruption on 24th October 2001 (from Planke et al, 2003, Photo by Phil Hardy, BBC 2001). b) Lokbatan mud volcano, Azerbaijan. The crater rim collapsed during the October 2011 eruption resulting in a large mud breccia flow that extended over the flanks for several hundred meters. c) Google Earth satellite image of the Turagay (left) and Kyagnizadag (right) mud volcanoes in Azerbaijan, d) Bledug Kuwu, sedimentary hosted hydrothermal system, Indonesia. Large bubbles of gas charged mud breccia continuously burst in the central part of the crater. e) Panoramic aerial view of the main active vent of the Lusi, sedimentary hosted hydrothermal system, East Java, Indonesia. f) Example of one of the powerful mud blasts during the Lusi geysering activity. g) Witkop III hydrothermal vent complexes, Karoo igneous province, South Africa. Example of eroded conduit of one of the numerous hydrothermal vent complexes formed after the emplacement of the early Jurassic igneous province. h) Examples of pipes and flow structures in the upper part of the palaeo hydrothermal vent complex Witkop III.

**Fig. 2:** Schematic drawing of different clastic piercement structures. a) mud volcano (modified after Mazzini, 2009) and b) a hydrothermal vent complex (modified after Jamtveit, 2004). Not to scale. In both cases, fluids are moving at depth through fractures and pores. The upper part of the system (mud volcano and hydrothermal vent complex) show rocks breccia and a lack of internal structure.

**Fig. 3:** Flow pattern map of air-water flows in a vertical pipe of 72 mm inner diameter, as a function of gas and liquid superficial density. (Modified after Taitel et al., 1980)

**Fig. 4**: Schematic evolution of the stream/water flow in a vertical boiler tube (modified after Brennen, 2005). Pressures and depths (left) at which flow-pattern transitions occur are estimated based on the gas volume ratio for an initial methane or carbon dioxide concentration of 1mol.kg$^{-1}$, a temperature of 60ºC and pressure from 0 to 500 bar.

**Fig. 5**: Typical flow curves that characterize the behaviour (shear stress) of a fluid when a progressive shearing deformation (shear rate) is applied to it. Bingham and Herschel-Bulkley fluid needs to excess a threshold stress (yield stress) for flow to take place. A Newtonian fluid shows a shear stress is linearly proportional to the shear rate.

**Fig. 6:** Schematic representation of a clastic piercement system with the main parameters and processes that control the dynamics of the eruption and that should be considered by models.

Figure

Click here to download high resolution image

Figure

Click here to download high resolution image

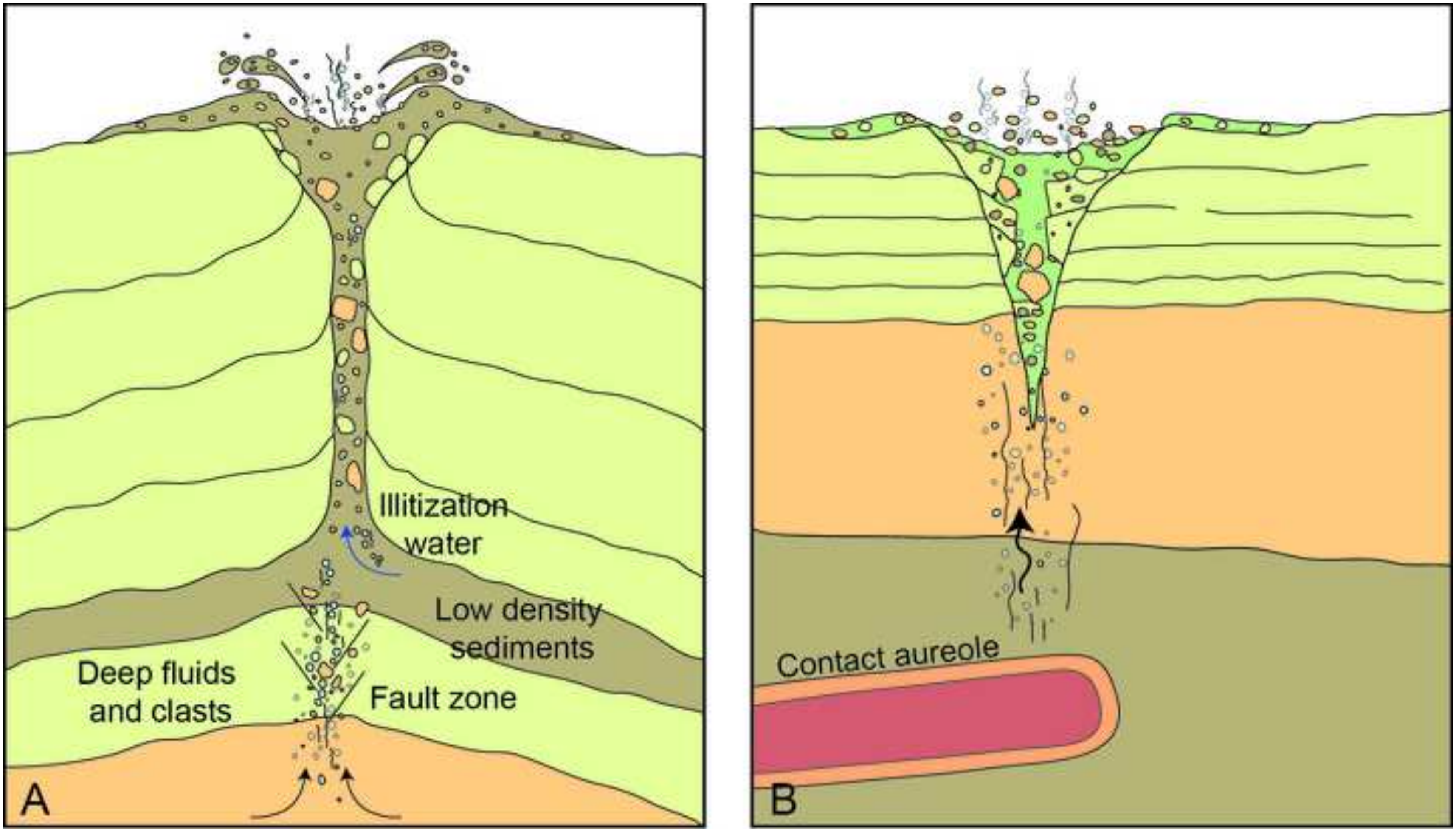

Figure
Click here to download high resolution image

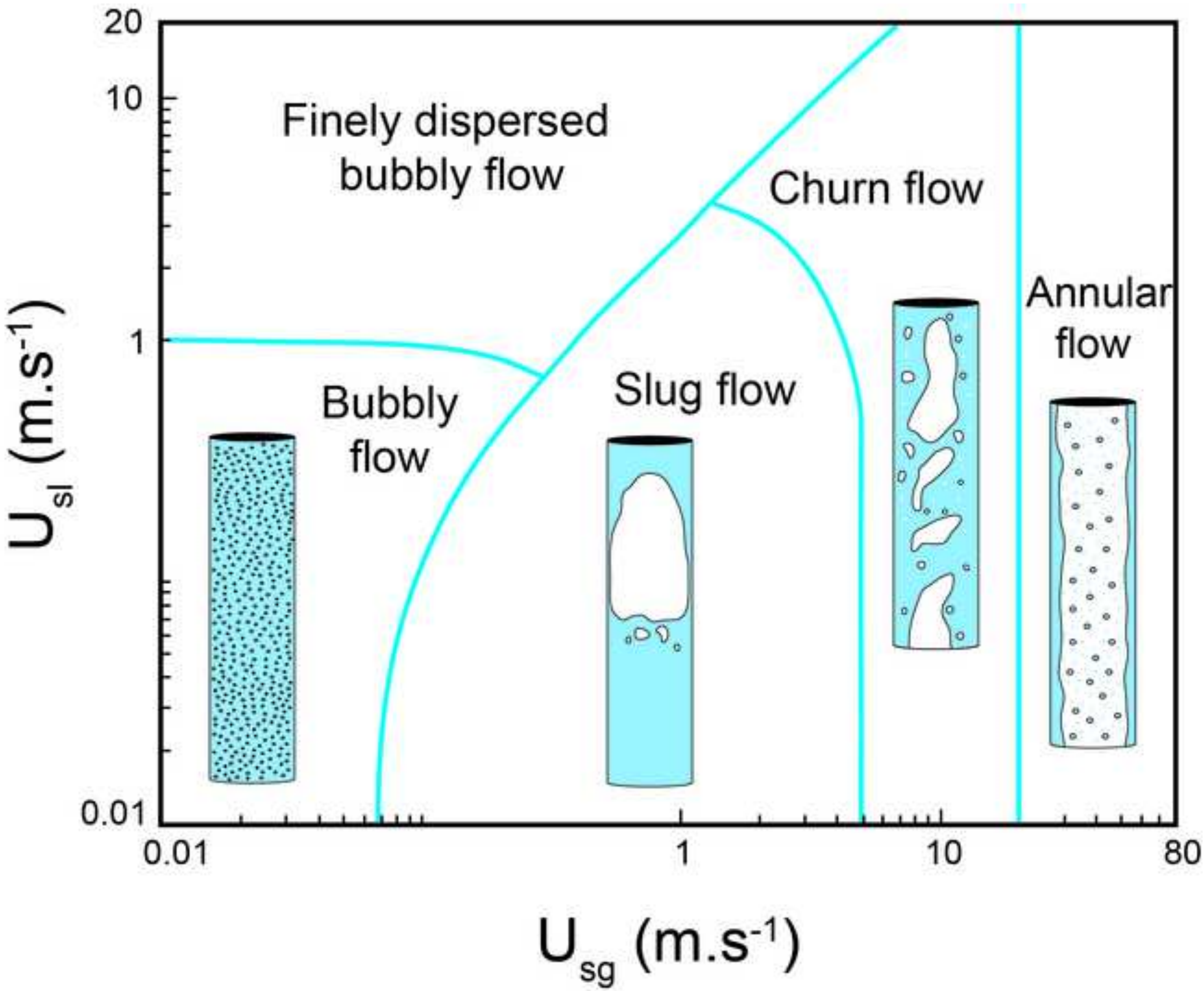

Figure
Click here to download high resolution image

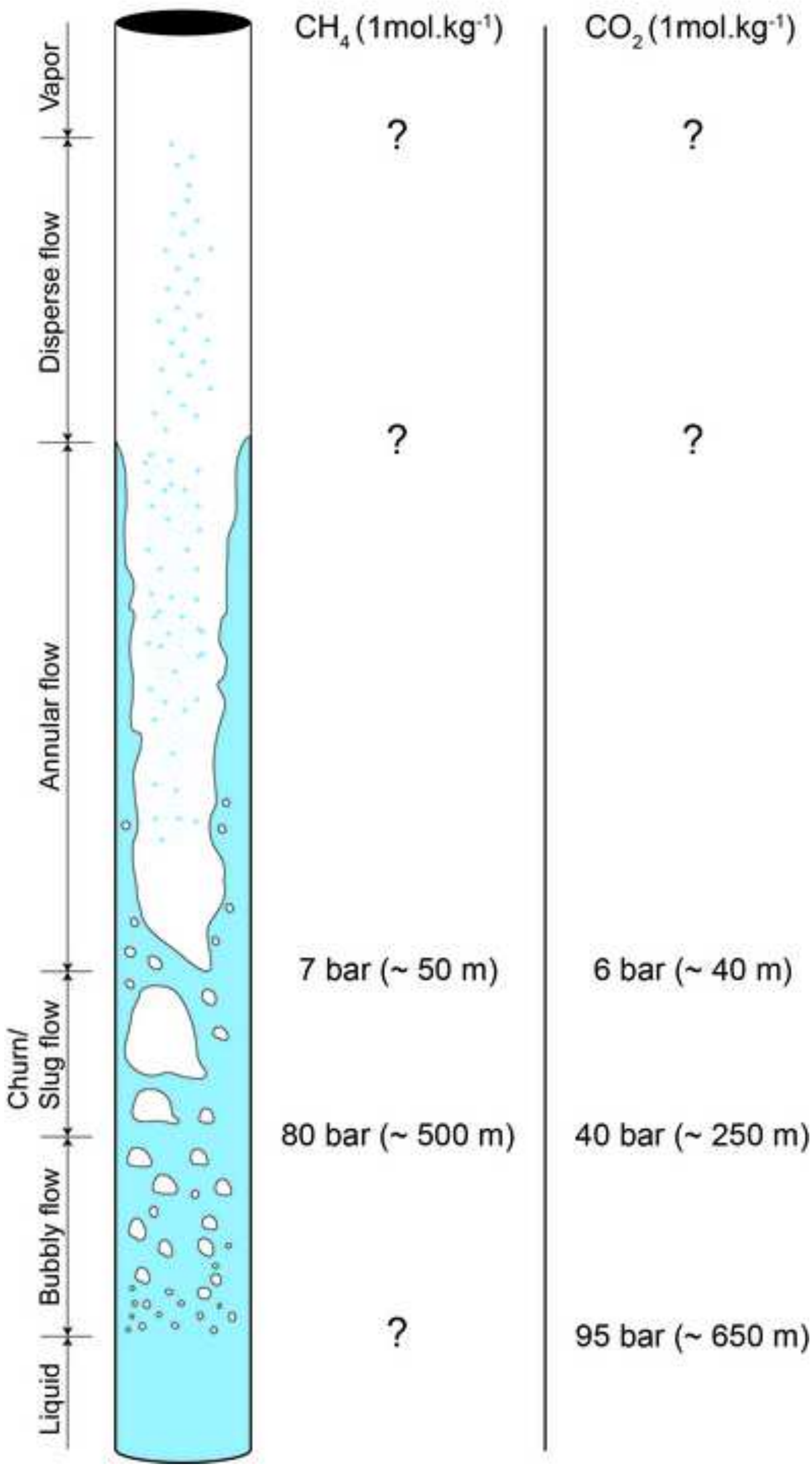

Figure
Click here to download high resolution image

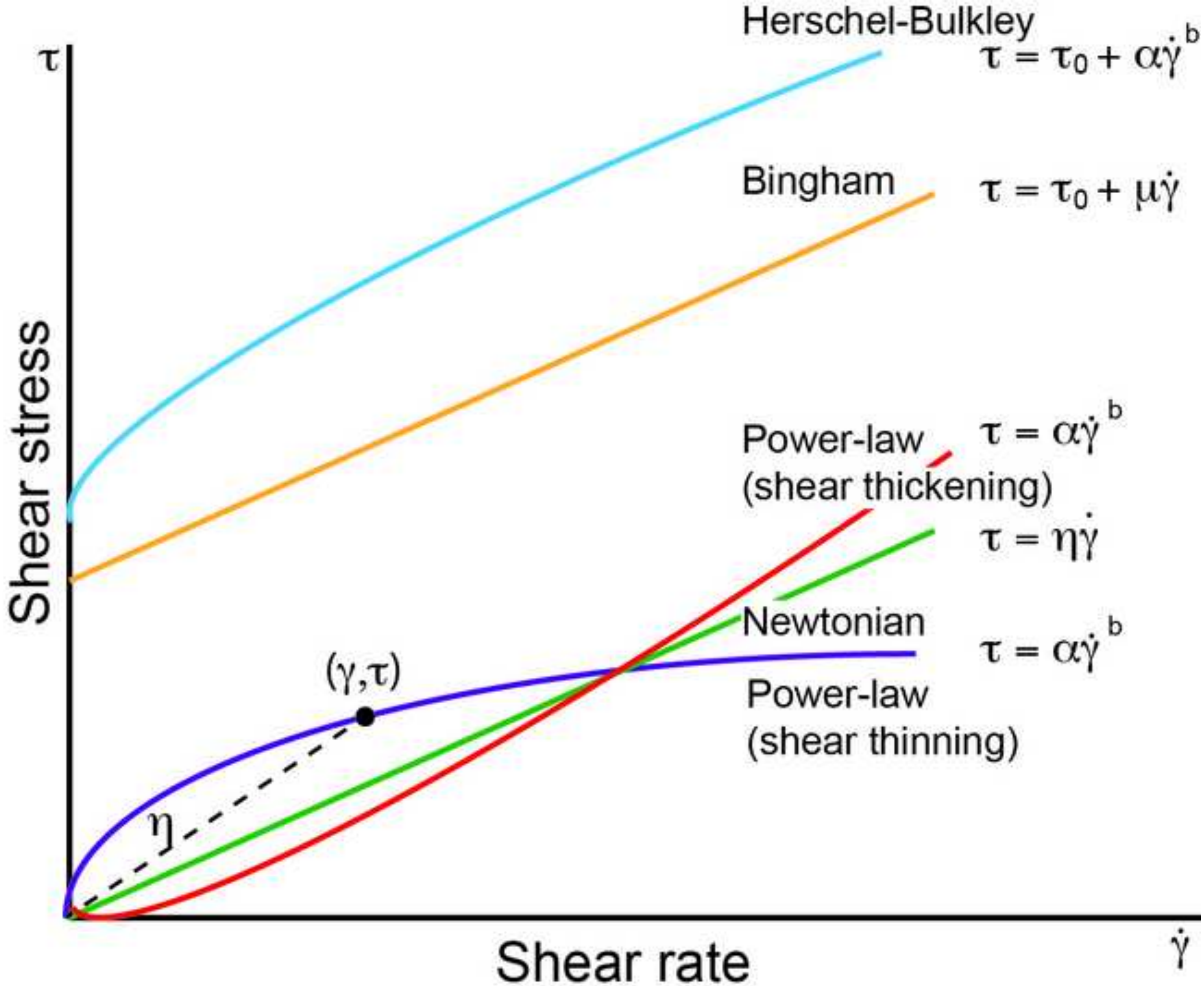

**Figure**

Click here to download high resolution image